Helsinki University of Technology
Department of Engineering Physics and Mathematics
Espoo 2003

CORTICAL DYNAMICS OF VISUAL FEATURE AND OBJECT-LEVEL PROCESSING IN THE HUMAN OCCIPITOTEMPORAL CORTEX: MEG SOURCE ANALYSIS AND EVALUATION OF CONDUCTIVITY MODELS

Antti Tarkiainen

Dissertation for the degree of Doctor of Science in Technology to be presented with due permission of the Department of Engineering Physics and Mathematics, Helsinki University of Technology for public examination and debate in Auditorium F1 at Helsinki University of Technology (Espoo, Finland) on the 28th of March, 2003, at 12 o'clock noon.

Helsinki University of Technology
Low Temperature Laboratory
Brain Research Unit

Teknillinen korkeakoulu
Kylmälaboratorio
Aivotutkimusyksikkö

Distribution:
Low Temperature Laboratory
Helsinki University of Technology
P.O. Box 2200
FIN-02015 HUT, Finland
Tel: +358-9-451 5619
Fax: +358-9-451 2969
This thesis is downloadable at http://lib.hut.fi/Diss/list.html

ISBN 951-22-6376-9 (printed version)
ISBN 951-22-6377-7 (electronic version)

Picaset Oy
Helsinki 2003

Title: Cortical dynamics of visual feature and object-level processing in the human occipitotemporal cortex: MEG source analysis and evaluation of conductivity models

Author: Antti Tarkiainen
Brain Research Unit, Low Temperature Laboratory
Helsinki University of Technology
P.O. Box 2200, FIN-02015 HUT, FINLAND
Email: antti.tarkiainen@hut.fi

Date: March, 2003

Abstract: The computer simulations carried out in this thesis demonstrated that a spherically symmetric conductor model is in most cases an adequate model for the conductivity geometry of the human head and the use of more sophisticated head models does not contribute considerably to the source estimation accuracy of magnetoencephalography. The main reason for this is the noise that is typically present in the measured signals and masks effectively the differences between different head conductor models. The brain activation studies carried out in this thesis concentrated on the early cortical processing of two special cases of behaviourally highly relevant and frequently encountered visual stimuli: letter-strings and faces. The results show that the early visual processing of both image types consists of at least two separable processes taking place in the occipital and occipitotemporal cortices within 200 ms after the stimulus presentation. The first process, associated with low-level visual feature analysis, occurred in the midline occipital cortex at about 100 ms after image onset. This processing stage was common to the analysis of both letter-strings and faces. From the occipital cortex the activity advanced to the inferior occipitotemporal areas bilaterally, reaching the maximum at about 150 ms after stimulus onset. Although both letter-strings and faces activated largely overlapping areas in the inferior occipitotemporal cortex, the hemispheric distribution of these areas was different. Letter-string processing concentrated to the left hemisphere, whereas face processing occurred more bilaterally, apparently with slight right-hemisphere dominance. This processing stage is likely to represent a more general object-level analysis phase that takes place after the common low-level analysis and acts as a gateway to higher processing areas. When these analysis stages were evaluated in dyslexic subjects a significant underactivation in the occipitotemporal cortex was found to letter-strings but not to faces. This result suggests that the dysfunction of occipitotemporal cortex previously reported in dyslexia is likely to be limited to the processing of letters or at least letter-like objects.

Keywords: Magnetoencephalography; MEG; conductor model; spherically symmetric model; realistically shaped model; current dipole; letter-string; word; face; object; noise masking; occipitotemporal; extrastriate; visual processing; dyslexia.

UDC: 612.82:616-073:004.94

Academic dissertation

Cortical dynamics of visual feature and object-level processing in the human occipitotemporal cortex: MEG source analysis and evaluation of conductivity models

Author: Antti Tarkiainen
Brain Research Unit
Low Temperature Laboratory
Helsinki University of Technology
Finland

Supervising professor: Professor Toivo Katila
Laboratory of Biomedical Engineering
Helsinki University of Technology

Supervisor: Professor Riitta Salmelin
Brain Research Unit
Low Temperature Laboratory
Helsinki University of Technology

Preliminary examiners: Docent Elisabet Service
Department of Psychology
University of Helsinki
Finland

Dr. Joachim Gross
Department of Neurology
Heinrich-Heine University
Düsseldorf
Germany

Official opponent: Dr. Anna Christina Nobre
University of Oxford
Department of Experimental Psychology
Brain & Cognition Laboratory
Oxford
United Kingdom

List of publications

This thesis consists of an overview and of the following six publications:

P1 **Tarkiainen A**, Liljeström M, Seppä M, and Salmelin R. (2003) The 3D topography of MEG source localization accuracy: effects of conductor model and noise. TKK report TKK-KYL-008.

P2 **Tarkiainen A**, Helenius P, Hansen PC, Cornelissen PL, and Salmelin R. (1999) Dynamics of letter string perception in the human occipitotemporal cortex. Brain **122**: 2119-2131.

P3 Helenius P, **Tarkiainen A**, Cornelissen P, Hansen PC, and Salmelin R. (1999) Dissociation of normal feature analysis and deficient processing of letter-strings in dyslexic adults. Cerebral Cortex **9**: 476-483.

P4 **Tarkiainen A**, Cornelissen PL, and Salmelin R. (2002) Dynamics of visual feature analysis and object-level processing in face versus letter-string perception. Brain **125**: 1125-1136.

P5 **Tarkiainen A**, Helenius P, and Salmelin R. (accepted for publication) Category-specific occipitotemporal activation during face perception in dyslexic individuals: An MEG study. NeuroImage.

P6 Cornelissen P, **Tarkiainen A**, Helenius P, and Salmelin R. (accepted for publication) Cortical effects of shifting letter-position in letter-strings of varying length. Journal of Cognitive Neuroscience.

Contributions of the author

All the publications included in this thesis are a result of group effort. I was the principal investigator and author in studies P1, P2, P4, and P5. I designed and performed the simulations and the source estimation in P1. I wrote the stimulus scripts and carried out the recordings and the main part of the signal analysis in P2. I was responsible for preparing the stimuli and the stimulus scripts and carrying out the MEG recordings and signal analysis in P4 and P5. I wrote the speed discrimination test algorithm for study P5 based on a previously published scheme. I also designed and wrote Matlab algorithms for some of the data analysis approaches used in these studies. I wrote the stimulus script and participated in preparing the manuscript for publication P3. I prepared the stimuli and stimulus script and contributed actively to the recordings, data analysis, and writing of publication P6.

Table of contents

Abbreviations

BEM	Boundary-element method
ECD	Equivalent current dipole
EEG	Electroencephalography
FEM	Finite element method
fMRI	Functional magnetic resonance imaging
FSA	Face-specific activation
LGN	Lateral geniculate nucleus
LSA	Letter-string-specific activation
MEG	Magnetoencephalography
MRI	Magnetic resonance image/imaging
PET	Positron emission tomography
SD	Standard deviation
SEM	Standard error of mean
SQUID	Superconducting quantum interference device
SSP	Signal-space projection
V1	Visual area 1, primary visual cortex
V2	Visual area 2
V2d	Visual area 2d
V3	Visual area 3
V3A	Visual area 3A
V3d	Visual area 3d
V4	Visual area 4
V5	Visual area 5
VFA	Visual feature analysis

Preface

The effort that has finally resulted in this thesis has mainly been fun. During the years, there has naturally been moments – like transferring helium into the neuromagnetometer during Christmas holidays or reading some quite extraordinary anonymous referee comments – when joy has not been the dominating feeling but these moments have been well overwhelmed and compensated by the happy moments shared with the great people of the Low Temperature Laboratory.

First, I would like to express my gratitude to the former and present leaders of the laboratory for all the work that they do behind the scenes so that we students can just come and use the excellent research facilities of the LTL without worries about the money. Academician Olli V. Lounasmaa, who unfortunately passed away a few months ago, was the driving force in creating the successful research unit known as the Low Temperature Laboratory. Even though he retired in 1995, he never really left the LTL and continued to contribute in his remarkable way to the daily life of the laboratory right until his untimely death. After Acad. Lounasmaa's retirement the laboratory has been steered insightfully by Prof. Mikko Paalanen who has done a great job in continuing the success story of the LTL.

Nowadays, Low Temperature Laboratory is at least equally well known for brain research as for research on different fields of low temperature physics and nanophysics. The biggest thank on the success and growth of the brain research belongs to Acad. Prof. Riitta Hari, the head of the Brain Research Unit of the laboratory. She is an amazingly energetic and knowledgeable person whose good-humoured character makes her a nice person to work with. I am very grateful that I have had this opportunity to work in the LTL.

The most influential and important individual contributing to the work I have done at the LTL is without doubt my supervisor Prof. Riitta Salmelin. I was a young student of physics when Prof. Salmelin welcomed me to the laboratory and during the last 8 years she has taught me everything I currently know about the human brain and how one can study it. She has always given me the support I need but also the breathing space that I require. It is safe to say that without her skillful guidance I would never have achieved the high goals I had set on my work. Thank you Riitta.

I am also in debt to all my other co-authors. Dr. Päivi Helenius has been an invaluable source of information both on dyslexia and on statistics. She has also served as my mentor amongst fellow students and shown me great personal example on how to write a good thesis. Dr. Piers Cornelissen has given me lots of good ideas, enthusiasm, and information that I have found precious during the years. In addition, he has also been a good friend with whom one can share comments on work and on life. Mika Seppä has been a valuable friend, a person to whom I have always been able to count for. I cannot but admire him for his many skills. Mia Liljeström has brought new ideas and energy to the laboratory and she did great work with the computer simulations presented here. Dr. Peter Hansen played an important role in the creation of the noisy letter-string stimuli.

I also want to thank my preliminary examiners Dr. Elisabet Service and Dr. Joachim Gross for their valuable comments and suggestions. I am also grateful to Prof. Toivo Katila, my supervisor on behalf of the Department of Engineering Physics and Mathematics, for his help during my studies and for motivating lectures on electromagnetic field theory.

Many of the everyday practicalities could not have gone as smoothly as they have without the great personnel of the LTL. Peter Berglund, Teija Halme, Marja

Holmström, Pirjo Kinanen, Tuire Koivisto, Satu Pakarinen, Liisi Pasanen, and the people of the liquefier and workshop make the laboratory work with the efficiency of a Swiss clock of highest standards. I want to express my warmest thanks to them all.

It has also been a great pleasure to work with so many nice colleagues at the LTL. They have all helped me in many ways and also made the laboratory such a pleasurable working environment. The expertise and many skills of doctors Matti Hämäläinen, Nina Forss, Ole Jensen, and Veikko Jousmäki have benefited me a lot. I am in gratitude to Sari Avikainen, Gina Caetano, Katri Cornelissen, Nobuya Fujiki, Samuli Hakala, Yevhen Hlushchuk, Mia Illman, Marianne Inkinen, Juha Järveläinen, Jaakko Järvinen, Helge Kainulainen, Ken-ichi Kaneko, Erika Kirveskari, Kari Kuukka, Hannu Laaksonen, Martin Lehecka, Sari Levänen, Karin Mårtenson, Jyrki Mäkelä, Jussi Numminen, Ritva Paetau, Marjatta Pohja, Antti Puurula, Tommi Raij, Tuukka Raij, Hanna Renvall, Miiamaaria Saarela, Timo Saarinen, Stephan Salenius, Ronny Schreiber, Martin Schürmann, Teija Silen, Topi Tanskanen, Claudia Tesche, Mikko Uusitalo, Simo Vanni, Nuutti Vartiainen, Minna Vihla, and Tiina Vuorinen and also to Matti Kajola, Samu Taulu, and the rest of the people of the Neuromag company for their friendship and support. I am also grateful to doctors Flamine Alary, Gabriel Curio, Reinhard König, Yung-Yang Lin, Nobuki Murayama, Nobuyuki Nishitani, Yoshio Okada, Stephen Swithenby, and many other visitors who have contributed to the atmosphere of the laboratory during the years.

Very special thanks go to Lauri Parkkonen and Kimmo Uutela, who have helped me in so many ways that I have lost the count already a long time ago, and to my hilarious roommates at ‘Siberia’: Cristina Simões and Jan Kujala, you have been Real Friends with capital letters.

I also want to thank the Human Frontier Science Program and the Finnish Graduate School of Neuroscience for the financial support of my work.

No work could be done if the rest of the life would be a mess. Fortunately, my private life has been far from a mess. I am in colossal debt to my parents Tuula and Simo, who have always given me their unconditional love and support. Last but certainly not least, I want to thank my wife Reeta for her smiles, love, understanding, support, back rubs, good meals, companionship – the whole package.

Espoo, February 2003

Antti Tarkiainen

Chapter 1

Introduction

All the information that we gather from our surroundings, as well as the actions that we plan and perform, are processed in the brain. Dysfunctions caused by brain lesions, diseases, or developmental abnormalities have been an important - and for a long time the only – source of information on the architecture and functions of the human brain. During the last decades, development of functional brain imaging methods has increased our knowledge about the brain and allowed research into brain function also in healthy individuals. In the work reported here, I have utilised one of these methods, magnetoencephalography, to study the visual processes involved in the analysis of letter-strings and faces both in non-reading-impaired adults and in dyslexic individuals, who have problems in reading (dyslexia).

By the onset of this project, both lesion and imaging studies had indicated that letters and faces are processed in specialised occipitotemporal areas, and electrophysiological studies had suggested that such stimulus-specific processing occurs at about 200 ms after letter-string/face presentation. MEG studies from our group had shown that in dyslexic individuals letter-strings did not activate the left inferior occipitotemporal cortex within the first 200 ms, an activation systematically detected in fluent readers. This finding was tentatively interpreted as impaired letter-string-specific processing in the dyslexic subjects, but it was essential to conduct further studies to identify the exact spatiotemporal sequence in letter-string perception and the functional roles of the cortical activation patterns.

The purpose of the studies presented in this thesis was to identify and characterise the spatiotemporal sequence of early letter-string processing and to compare that sequence in fluently reading and dyslexic adults. An additional goal was to determine when and where the cortical processing of letter-strings starts to differ from that of faces. Furthermore, cortical dynamics of face processing in dyslexia were investigated to test whether the early deficit in letter-string processing reflects a more general impairment in category-specific analysis.

The results presented here demonstrate that the early visual processing of letters and faces consists of at least two separable stages. The first cortical processing stage that my collaborators and I were able to identify through manipulation of stimulus parameters reflected low-level visual feature analysis that takes place in the occipital cortex at about 100 ms after the appearance of the stimulus image. This processing stage was common to both face and letter-string processing and it showed no difference between fluent and dyslexic readers. About 30 – 50 ms later, the brain processing segregated to stimulus-specific routes where letter-strings were processed mainly in the left inferior occipitotemporal cortex and face information in the same or immediately adjacent areas but bilaterally, with slight right-hemisphere preponderance. At this object-level processing stage, we detected the first differences between fluent and dyslexic readers: the letter-string-specific activation in the left hemisphere, systematically observed in fluent readers, was weak or undetectable in most of the dyslexic subjects. The corresponding face-specific responses were, however, similar in both subject groups implying that the dysfunction of the left

occipitotemporal areas in letter-string processing is not related to cortical area or time-window of activation *per se*, but is more specific to the type of information being processed.

The strong point of magnetoencephalography (MEG) is the temporal resolution that allows tracking brain activations with millisecond time resolution. With MEG it is also possible to localise the measured activations with relatively good spatial accuracy. This task is, however, complicated by the nature of the electromagnetic signals themselves and requires the use of models that estimate the conductivity geometry of the head as well as the currents flowing in the brain. The methodologically simplest and most widely used conductor model is a sphere, which also reflects rather well the true geometry of the human brain. The rapid development of computer technology has facilitated the use of more complex and more realistic models as well. In one of the studies reported here, I investigated the properties of different types of conductor models and their effectiveness in localisation of brain activity.

Chapter 2

Magnetoencephalography

Information transfer between neurons results in small electric currents and, accordingly, to tiny electromagnetic fields. Magnetoencephalography (MEG) is a method where brain function is studied by measuring the evoked magnetic fields outside the head. Due to the weakness of the signals, MEG is technically very demanding. Also, the modelling of the measured activation requires sophisticated methods and tools as well as information about the underlying physiology of the human brain. In the following chapters I will describe the basic concepts ranging from the origin of the MEG signals to the modelling of the measured activity, with special emphasis on the hardware and methods used in the publications P1 to P6. A more detailed description of many of the issues discussed here can be found in the extensive MEG review by Hämäläinen et al. (1993).

2.1 Origin of neuromagnetic fields

Neurons are the main building blocks of the huge network that processes information and relays signals in the brain. A neuron (Fig. 2.1) consists of a cell body called soma, afferent branches called dendrites, and an efferent branch called axon. About 10^{10} neurons (Williams and Herrup, 1988) are located in the cortex, which is a layer of about 2 – 4 mm in thickness. The area of the cortex in a human is about 2500 cm^2 but because the cortex is strongly folded it fits inside the skull even though the area of the inner surface of the cranium is only about 700 cm^2.

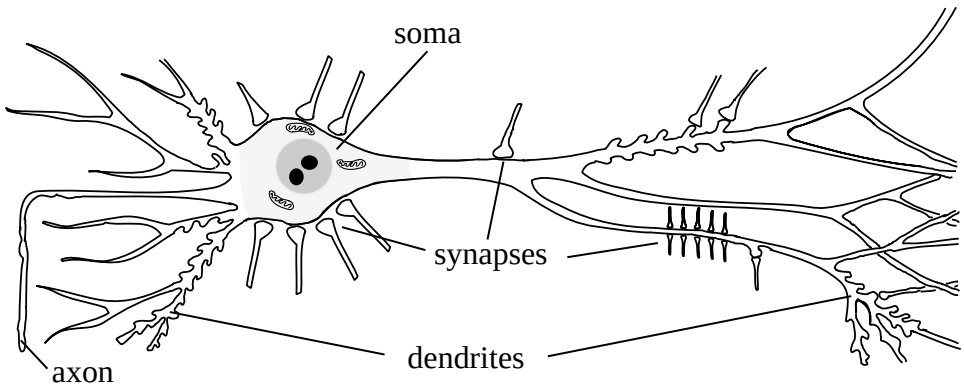

Fig. 2.1 Schematic illustration of a pyramidal neuron. Information from one neuron to another is conveyed across synapses. If the net effect of the postsynaptic potentials depolarises the cell enough, the neuron will fire an action potential that will travel along the axon. Modified from Iversen (1979).

The neurons' ability to convey signals is based on the functioning of the cell membrane. The proteins located in the membrane act as active and passive gateways for different types of ions. The most important active gateway is the Na-K-pump that conveys Na^+ ions out of the cell and K^+ ions from outside to the inside of the cell thus creating a concentration difference between the inner and outer volumes. This difference causes diffusion through the ion channels that results in movement of a net charge. The resulting potential difference opposes the flow of ions and equilibrium is reached when currents created by diffusion and potential difference cancel each other. In resting condition the potential in the cell is about –70 mV with respect to the outside of the cell.

If the cell is depolarised, i.e. the potential difference is decreased, voltage sensitive Na^+ channels open and Na^+ ions start to flow into the cell increasing depolarisation further. This affects also nearby ion channels, which open up, creating a travelling constant amplitude voltage pulse called an action potential. An action potential lasts only for one millisecond because voltage sensitive K^+-channels quickly open up and repolarise the cell.

From one neuron to another the signal is conveyed across a synapse. This happens usually with the help of chemical transmitters. When the action potential reaches the synaptic cleft in the presynaptic cell, transmitters are released into the synaptic cleft. Transmitter molecules affect the potential of the postsynaptic cell by either repolarisation (inhibitory synapse) or depolarisation (excitatory synapse). The net effect of all the synapses determines whether the postsynaptic cell will fire an action potential or not. The excitatory synapses are usually located in the dendrites and inhibitory synapses close to the soma.

The postsynaptic potential caused by the net effect of synapses can last for several tens of milliseconds, which enables the temporal summation of postsynaptic potentials in neighbouring, parallelly oriented neurons. The magnetic signals that can be measured outside the head using magnetoencephalography are usually generated by postsynaptic currents and especially in large pyramidal neurons that are oriented perpendicular to the surface of the cortex, with many parallel dendrites. A detectable signal is created by synchronous activation of thousands of neurons, which in practice may correspond to an activated cortical area of about 40 – 250 mm^2 (Chapman et al., 1984; Hari, 1990). MEG typically does not detect the electric current associated with the propagating action potential due to its short duration and quadrupolar formation.

2.2 Measurement of magnetic fields

2.2.1 SQUIDs and pickup coils

The magnetic signals generated in the brain and recorded outside of the head are very weak, typically in the order of 50 – 500 fT, which is only $1/10^9$ – $1/10^8$ of the static geomagnetic field of the Earth. However, these tiny signals can be measured using SQUID (superconducting quantum interference device) sensors (Zimmerman and Silver, 1966; Ryhänen et al., 1989). The operation of a SQUID is based on superconductivity. Therefore, the sensors have to be stored in liquid helium.

A SQUID sensor is formed of a superconducting loop that is interrupted by one (RF-SQUID) or two (DC-SQUID) thin, insulating junctions, called Josephson junctions (Josephson, 1962). When a SQUID sensor is used to measure a magnetic field, the external field couples to the SQUID loop via a flux transformer that consists

of a pickup coil and a signal coil. This setup is illustrated in Fig. 2.2a. Changes in the magnetic flux (Φ_a) passing the SQUID loop change the impedance of the loop. These changes can be measured by feeding a bias current (I_b) to the loop and by measuring the voltage across it (V). The measured voltage is a periodic function of the flux (Fig. 2.2b). Because of this, the measurement of the voltage V would enable the measurement of flux changes of only one period (Φ_0), which is not adequate. This problem is resolved by feeding the detected signal back to the SQUID loop so that the flux changes caused by the measured external field are cancelled and the SQUID remains locked to its working point. By measuring the required feedback current one can determine the strength and time behaviour of the measured magnetic field.

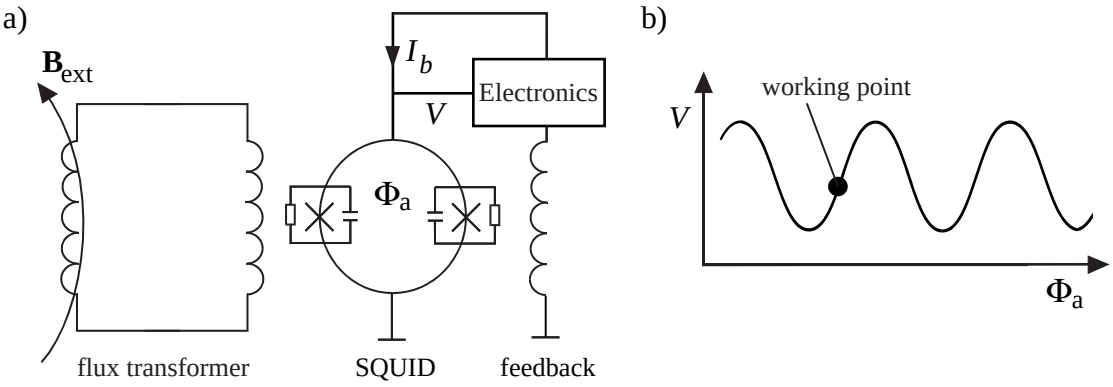

Fig. 2.2 A DC-SQUID sensor and its characteristic curve. a) The external magnetic field $\mathbf{B}_{ext}$ is connected to the SQUID loop via a flux transformer. The voltage V depends on the bias current I_b and on the magnetic flux (Φ_a) penetrating the SQUID loop. The two Josephson junctions are marked with X. b) Voltage V depends periodically on the flux going through the SQUID. The feedback circuitry is used to keep the flux through the SQUID loop constant, locking the SQUID to its working point.

The properties of a SQUID-based measurement sensor can, to a considerable extent, be controlled by the design of the pickup coil. A magnetometer is a sensor that has a simple one loop pickup coil (Fig. 2.3a). Magnetometers are more sensitive to magnetic fields from far away sources than other pickup coil designs, which may be beneficial for studying deep brain structures, but, on the negative side, they are also more sensitive to noise sources. A different spatial sensitivity pattern can be achieved using a gradiometer where the pickup coil consists of two or more loops in a planar or axial configuration. This design is most sensitive to magnetic fields from nearby sources and results in effective noise cancellation as the practically homogeneous fields created by far away sources such as electric cables and motors induce equal but opposite currents in the loops. A first-order planar gradiometer is illustrated in Fig. 2.3b.

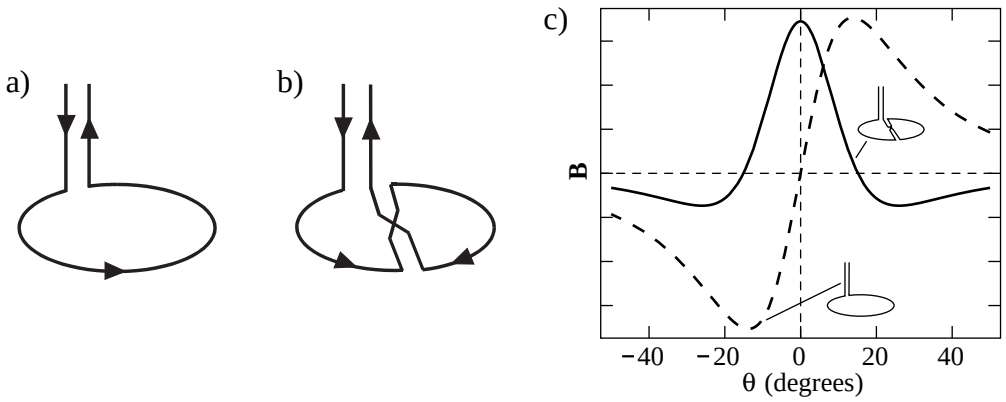

Fig. 2.3 Examples of pickup coil design. a) A magnetometer is a simple loop. b) A first-order planar gradiometer has a double-D construction. c) If the magnetic field **B** generated by a current dipole at location 0 degrees is being measured, a planar gradiometer measures the maximal signal (solid line) just above the source whereas a magnetometer picks up the strongest signals (dashed line) on both sides of the source. Adapted from Hämäläinen et al. (1993).

2.2.2 Neuromagnetometers

A neuromagnetometer is a device that typically consists of a large number of SQUID sensors in a grid formation that is designed for recording of brain activations (Fig. 2.4a). The studies presented in this thesis were carried out with two different neuromagnetometers. Data in the studies P2 and P3 were measured with the 122-channel Neuromag-122™ device (Knuutila et al., 1993) and in the studies P4, P5, and P6 with the newer 306-channel Vectorview™ system, both prototypes of devices manufactured by the Neuromag company (Neuromag Ltd, Helsinki, Finland). Also, the simulations presented in the study P1 were calculated for the sensor grid of the Vectorview™ system. In both systems DC-SQUID sensors are distributed in a helmet-shaped array that can simultaneously record signals from the whole cortex (Figs. 2.4b and c).

In Neuromag-122™ all the 122 sensors (Fig. 2.4b) are first-order planar gradiometers, similar to those illustrated in Fig. 2.3b. They are distributed into 61 locations so that two orthogonal gradiometers are always located at each position. The sensor array of the Vectorview™ system consists of 102 magnetometers and 204 first-order planar gradiometers distributed into 102 locations, each containing one magnetometer and two orthogonal gradiometers (Fig. 2.4c).

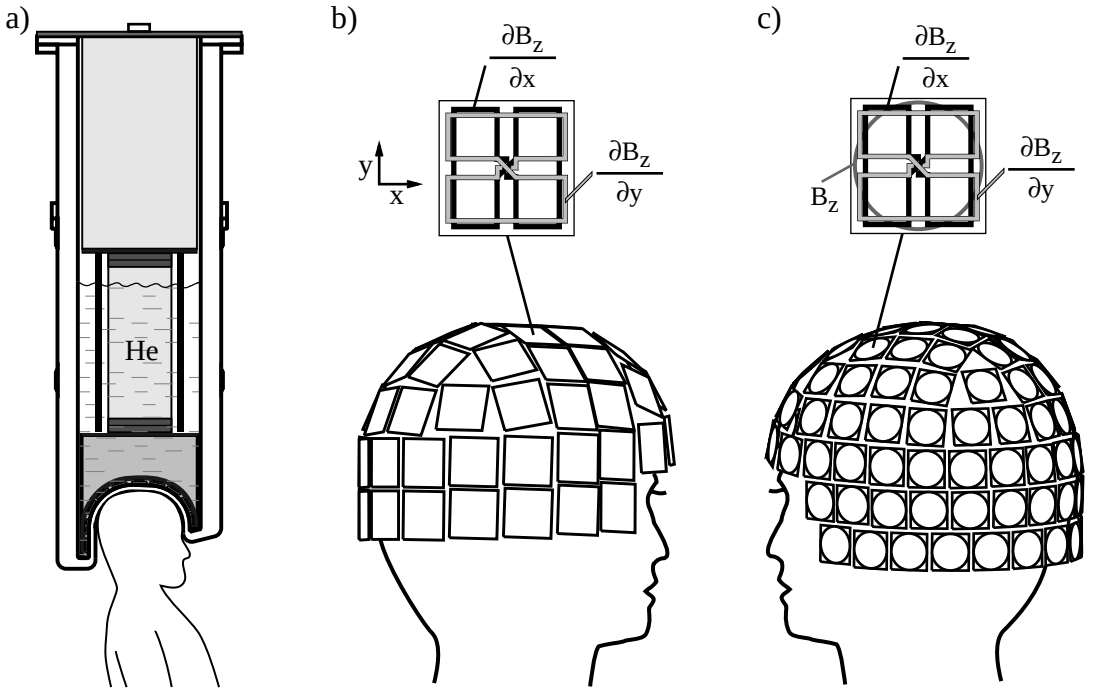

Fig. 2.4 Examples of neuromagnetometer design. a) The Neuromag-122™ magnetometer contains liquid helium to keep the SQUID sensors in superconducting state. The subject's head is placed under the helmet-shaped sensor array. b) The sensor-array of Neuromag-122™ contains 61 recording sites, each with two first-order planar gradiometers that measure the change of the magnetic field component normal to the sensor surface (B_z) along two orthogonal directions. c) The Vectorview™ system has 102 recording sites, each with two orthogonal gradiometers similar to Neuromag-122™ but also with an additional magnetometer. The pickup coil configuration is a simplified illustration and not the exact design (adapted partly from Hämäläinen et al., 1993).

2.2.3 MEG recordings

In a typical MEG recording session, like in studies P2, P3, P4, P5, and P6, the subject is presented with a series of stimuli and s/he has a specific task related to them. For example, in study P2 the subject was asked to view presented letters and letter-strings and, after seeing an occasional question mark, s/he had to name the letter or letter-string that was shown just before it. The purpose of a task like this is often to make sure that subjects pay attention to the stimulus presentation. In many cases the subject's responses can also be used to evaluate the difficulty of the task or the subject's performance. In addition to evoked responses, phase-locked to presentation of a specific stimulus type or onset of task performance, task-related modulation of spontaneous brain rhythms can be recorded and studied as well (see e.g. Salmelin and Hari, 1994; Salenius et al., 1995; Hari and Salmelin, 1997).

To prepare the subject for a MEG recording, the experimenter explains the experimental procedure and the task and fixes a small number of electrodes and coils to the subject. The purpose of the electrodes is to monitor possible sources of artefacts and muscle movements. The most typical artefacts are caused by eye movements. The magnetic fields created by eye blinks and saccades are so large that they will mask the

brain activations of interest. Therefore, it is important that all brain responses contaminated by them are excluded from the data analysis. Another use for electrodes is the monitoring of subject's task-related activities, e.g. lifting of a finger and opening of the mouth during speech.

The purpose of the coils is to allow the determination of the subject's head position with respect to the SQUID sensor array. This information is vital for the accurate localisation of the recorded brain activity. Before the actual MEG recording, three or four coils are attached to the subject's head. Their locations are measured with a 3D digitiser with respect to anatomical landmarks that can also be reliably identified from anatomical magnetic resonance images (MRIs) of the subject. The landmarks used in our studies were the points just anterior to the ear canals and the nasion. These points also define the head coordinate system where the *x*-axis runs through the points anterior to ear canals from left to right, the positive *y*-axis runs through the nasion and the *z*-axis is perpendicular to both the *x*- and *y*-axes and runs towards the top of the head (Fig. 2.5). At the beginning of the MEG measurement, the coils are energised briefly and the resulting magnetic field is measured. This allows the coils to be located with respect to the sensor array of the neuromagnetometer. Because the coil locations are also known with respect to the anatomical landmarks, all MEG measurement results can be transformed into the head coordinate system and aligned with anatomical images. Lately, it has also become possible to obtain continuous head location information (Uutela et al., 2001).

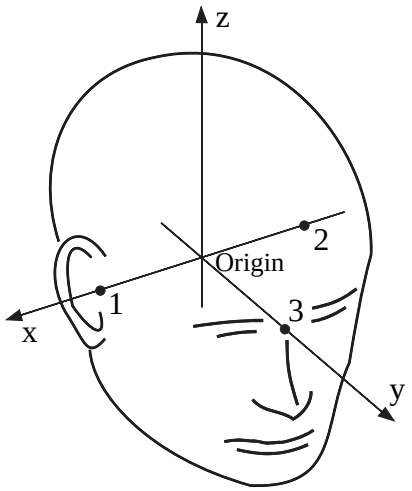

Fig. 2.5 Definition of the head coordinate system used in our MEG recordings. The points anterior to ear canals (1, 2) define the *x*-axis. The *y*-axis is perpendicular to the *x*-axis and passes through the nasion (3). The *z*-axis is perpendicular to both the *x*- and *y*-axes and runs through the origin defined by their intersection.

2.2.4 Reduction of noise

Because the magnetic fields evoked by neural currents are extremely weak, it is important that all the magnetic fields that interfere with the measurement and analysis of the brain activation of interest, and can therefore be considered as noise, are attenuated as much as possible. Here, the definition of noise does not include only interfering fields from nearby electric cables, motors, passing cars etc. and noise

caused by the measurement hardware but also signals that originate from the subject. Such fields are created by small movements of magnetic objects in subject's clothing, by eye movements and blinks, by muscle (especially heart) contractions, and by brain activity that is not related to the studied phenomenon (see e.g. Jousmäki, 1998; Hari, 1999).

To reduce the magnetic noise from the environment, the MEG recordings are normally carried out in a magnetically shielded room, where the walls are typically made of layers of aluminium and μ-metal (see e.g. Kelhä et al., 1982). The external noise fields can also be diminished by the use of active shielding, i.e. by measuring the external fields and creating equal but opposite fields that cancel the noise (Holmlund et al., 2001).

The signal-to-noise ratio can be improved significantly by collecting several brain responses evoked by a certain stimulus type and averaging them together. This procedure enhances the responses that are phase-locked to the stimulus presentation, i.e. repeat themselves in a similar way, and attenuates responses that are not systematically linked to the stimulus presentation. However, it is often wise to keep the number of averages collected as small as possible as long recording sessions can fatigue the subject and alter the brain responses.

The effect of many noise components, especially the always present 50-Hz noise from the mains current, can also be decreased by filtering the data and by applying sophisticated techniques such as the signal-space projection (SSP; see e.g. Uusitalo and Ilmoniemi, 1997). As mentioned in chapter 2.2.1, additional noise reduction can be achieved by using SQUID sensors with e.g. planar gradiometers instead of magnetometers. The impact of noise on the source estimation accuracy is considered in the publication P1.

2.3 Source modelling

The purpose of many MEG studies is to reveal the spatiotemporal pattern of activation related to some specific sensory or cognitive operation performed by the subject. This is done by solving the inverse problem of neuromagnetism, i.e. by locating the activated brain areas based on the measured magnetic field, and by modelling their time behaviour. The process first requires solving the forward problem, i.e. calculation of the resulting magnetic field outside the head when the current distribution inside the brain is known.

The calculation of the magnetic field outside the head requires models that mimic the conductor geometry of the head and the currents flowing in the brain. Typical conductor models include spherically symmetric conductors and more realistically shaped boundary-element models that follow the true shape of the brain, and possibly also that of the skull and scalp, with different but constant conductivities for the different compartments. The most widely used model for the neural activation is a point-like current dipole.

A solution to the inverse problem can be found using iterative methods. When the conducting volume and the current distribution are represented with appropriate models, an initial guess can be made and the resulting magnetic field (forward problem) can be calculated. The parameters of the current distribution model are then varied in order to minimise the difference between the recorded field and predicted field. The goal of this procedure is to find a current distribution that accounts for the measured magnetic field patterns.

The inverse problem is often ill-posed because large changes in model parameters may yield only small changes in the measured field. Also, several different current distributions can generate the same electromagnetic fields outside the head (Helmholtz, 1853). To overcome the problem of non-uniqueness one has to set some constraints, which requires the use of *a priori* physiological and anatomical information. Typical assumptions restrict the number of simultaneously active sources, the strength of the current flowing in the brain, and/or the acceptable source locations. Therefore, the physiological validity of the resulting activation model can only be evaluated with experience and prior knowledge about the functioning of the brain.

2.3.1 Maxwell's equations

The starting point for the calculation of the forward problem is given by Maxwell's equations that govern the electromagnetic field. Assuming that the permeability of the tissue μ is equal to the permeability of the vacuum μ_0, Maxwell's equations read

$$\begin{aligned} \nabla \cdot \mathbf{E} &= \rho / \varepsilon \\ \nabla \times \mathbf{E} &= -\partial \mathbf{B} / \partial t \\ \nabla \cdot \mathbf{B} &= 0 \\ \nabla \times \mathbf{B} &= \mu_0 (\mathbf{J} + \varepsilon \partial \mathbf{E} / \partial t), \end{aligned} \tag{2.1}$$

where **E** stands for electric field, **B** denotes magnetic field, ρ total charge density, ε permittivity, t time, and **J** total current density.

Because most of the bioelectromagnetic signals are below 1000 Hz, it can be shown that the time-derivative terms in Eq. 2.1 are negligible and can be ignored (Hämäläinen et al., 1993). According to this quasistatic approximation, Maxwell's equations take the simplified form

$$\begin{aligned} \nabla \cdot \mathbf{E} &= \rho / \varepsilon \\ \nabla \times \mathbf{E} &= 0 \\ \nabla \cdot \mathbf{B} &= 0 \\ \nabla \times \mathbf{B} &= \mu_0 \mathbf{J}. \end{aligned} \tag{2.2}$$

Because $\nabla \times \mathbf{E} = 0$, the electric field can be described with the help of a scalar potential V:

$$\mathbf{E} = -\nabla V. \tag{2.3}$$

It is also customary to divide the total current density **J** into two components:

$$\mathbf{J} = \mathbf{J_p} + \mathbf{J_v}. \tag{2.4}$$

The primary currents $\mathbf{J_p}$ flowing inside or close to a cell are caused by the neural activity whereas volume currents, $\mathbf{J_v} = -\sigma \nabla V$, are ohmic currents, governed by the macroscopic conductivity σ and macroscopic electric potential, that flow passively

everywhere in the medium. Finding the primary current $\mathbf{J_p}$ capable of explaining the measured field solves the inverse problem.

2.3.2 Calculation of the magnetic fields

When the total current density is known, a magnetic field fulfilling Maxwell's equations 2.2 can be calculated from the Ampere-Laplace's law

$$\mathbf{B}(\mathbf{r}) = \frac{\mu_0}{4\pi}\int \frac{\mathbf{J}(\mathbf{r}')\times(\mathbf{r}-\mathbf{r}')}{|\mathbf{r}-\mathbf{r}'|^3}dv', \tag{2.5}$$

where **r** denotes the location where the magnetic field is calculated and **r**' denotes the source coordinates within the brain. Combining equations 2.2, 2.4, and 2.5 gives (Hämäläinen et al., 1993)

$$\mathbf{B}(\mathbf{r}) = \frac{\mu_0}{4\pi}\int (\mathbf{J_p} + V\nabla'\sigma)\times\frac{(\mathbf{r}-\mathbf{r}')}{|\mathbf{r}-\mathbf{r}'|^3}dv' \tag{2.6}$$

and

$$\nabla\cdot(\sigma\nabla V) = \nabla\cdot\mathbf{J_p}, \tag{2.7}$$

which create the basis for solving the forward problem. The calculation of the magnetic field **B** requires information on both the primary current $\mathbf{J_p}$ and on the macroscopic conductivity geometry $\sigma(\mathbf{r})$.

2.3.3 Current dipole model

Different current distribution models can be used to describe the primary currents generated in the brain. A simple, but also a very practical model is given by a point-like current dipole with specific location, orientation, and strength (Williamson and Kaufman, 1981; Tuomisto et al., 1983). The current dipole **Q** at location $\mathbf{r_Q}$ can be defined with the help of Dirac's delta function:

$$\mathbf{J_p}(\mathbf{r}) = \mathbf{Q}\delta(\mathbf{r}-\mathbf{r_Q}). \tag{2.8}$$

The current dipole model is justified if the active source area is not large compared with the distance to the measurement sensors, which in practice is often the case. The field patterns evoked by pyramidal neurons have typically a very dipolar appearance, so a current dipole is in many cases a reasonable and physiologically meaningful model for the activity. To account for the spatiotemporal pattern of activity measured over the entire brain and/or longer time windows, one can construct a so-called multi-dipole model where each dipole represents activity observed at one location and within a certain time range. The parameters of the dipoles explaining the measured magnetic fields can be estimated with user intervention one at a time until a reasonable model has been obtained or by using more automated techniques (see e.g.

Mosher and Leahy, 1999). A more detailed description of the strategies applied in the studies included in this thesis can be found in connection with each publication.

In addition to current dipole models where a small number of dipole locations are determined based on the measured data, the inverse problem can be approached with continuous or distributed source models (see e.g. Ioannides et al., 1990; Dale and Sereno, 1993; Hämäläinen and Ilmoniemi, 1994; Pascual-Marqui et al., 1994; Gorodnitsky et al., 1995; Gross and Ioannides, 1999; Uutela et al., 1999).

2.3.4 Spherically symmetric conductor model

The analytically solvable spherically symmetric model is the most often used conductor model in MEG. In a spherically symmetric model the conductivity $\sigma = \sigma(r)$ depends only on the distance from the sphere origin. In addition to its mathematical simplicity, the sphere model is also meaningful as many parts of the brain follow the shape of a sphere reasonably well.

The magnetic field created by currents inside a spherically symmetric conductor can be calculated from Eq. 2.5. Because volume currents do not affect the radial component of the magnetic field, $B_r = \mathbf{B}(\mathbf{r}) \cdot \mathbf{e}_\mathbf{r}$ (Hämäläinen et al., 1993), Eq. 2.5 can be written as

$$B_r(\mathbf{r}) = \frac{\mu_0}{4\pi} \int \frac{\mathbf{J_p}(\mathbf{r}') \times (\mathbf{r} - \mathbf{r}')}{|\mathbf{r} - \mathbf{r}'|^3} \cdot \mathbf{e}_\mathbf{r} dv', \tag{2.9}$$

from where it can also be seen that B_r vanishes for any radial primary currents. According to Maxwell's equations, $\nabla \times \mathbf{B} = 0$ outside the conductor, so $\mathbf{B}$ outside of the head can be derived from a magnetic scalar potential U as $\mathbf{B} = -\mu_0 \nabla U$.

Because $\nabla \cdot \mathbf{B} = 0$ (Eq. 2.1), U can be determined uniquely when we know its normal derivative on the surface of the conductor volume and demand that it vanishes for $r \to \infty$, which gives (Hämäläinen et al., 1993)

$$U(\mathbf{r}) = \int_{t=1}^{\infty} B_r(t\mathbf{r}) dt. \tag{2.10}$$

The magnetic field $\mathbf{B}$ outside a spherically symmetric conductor can thus be determined without knowing the conductivity profile $\sigma = \sigma(r)$. It is also important to note that radial primary currents do not create magnetic fields outside of the sphere. Because of the sphere-like shape of the head MEG is most sensitive to tangential currents, which – taking into account that pyramidal neurons are oriented perpendicular to the surface of the cortex – means that the major contribution to magnetic fields measured outside the head comes from fissural cortex. Luckily, due to the folded structure of the cortex, about 2/3 of the cortical surface is located within the fissures.

2.3.5 Realistically shaped conductor model

A more realistic description of the head conductor geometry can be achieved by using realistically shaped conductor models. These models utilize anatomical information

obtained typically from MRIs. Because the conductivity of the skull is small compared with that of the brain tissue, the currents flowing in the skull and the scalp are small. For the calculation of the magnetic fields, it is thus often adequate to describe the head with a single-compartment model approximating the shape of the brain, or more specifically, the shape of the intracranial space (Hämäläinen and Sarvas, 1989). However, for a more detailed description of the head, also multi-compartment models may be applied. In contrast to the spherical model, the magnetic field in a realistically shaped model cannot be calculated analytically but numerical methods have to be used.

In a piecewise homogeneous conductor $\nabla\sigma$ is nonzero only at the boundaries. The magnetic field can then be written as (Geselowitz, 1970)

$$\mathbf{B}(\mathbf{r}) = \mathbf{B_0}(\mathbf{r}) + \frac{\mu_0}{4\pi}\sum_{i,j}(\sigma_i - \sigma_j)\int_{S_{ij}} V(\mathbf{r}')\frac{(\mathbf{r}-\mathbf{r}')}{|\mathbf{r}-\mathbf{r}'|^3}\times d\mathbf{S}' \qquad (2.11)$$

where $\mathbf{B_0}$ is the magnetic field created by the primary current $\mathbf{J_p}$, σ_i is the conductivity of the homogeneous compartment *i* and S_{ij} is the boundary between compartments *i* and *j*. As indicated by the above equation, the computation of the magnetic field requires knowledge of the potential on the surfaces of the compartments. The potential *V* can be calculated from (Barnard et al., 1967; Geselowitz, 1967)

$$V(\mathbf{r}) = \frac{\sigma_0}{\sigma(\mathbf{r})}V_0(\mathbf{r}) - \frac{1}{4\pi}\sum_{i,j}\frac{(\sigma_i-\sigma_j)}{\sigma(\mathbf{r})}\int_{S_{ij}} V(\mathbf{r}')\frac{(\mathbf{r}-\mathbf{r}')}{|\mathbf{r}-\mathbf{r}'|^3}\times d\mathbf{S}', \qquad (2.12)$$

where σ_0 denotes the unit conductivity $(\sigma_0 = 1/(\Omega\mathrm{m}))$ and

$$V_0(\mathbf{r}) = \frac{1}{4\pi\sigma_0}\int\frac{\nabla'\cdot\mathbf{J_p}}{|\mathbf{r}-\mathbf{r}'|}dv' \qquad (2.13)$$

is the potential that the primary currents create in unbounded medium with unit conductivity.

A realistically shaped brain model can be defined using the boundary-element method (BEM) where the shape of each compartment (in single-compartment models the brain and in 3-layer multi-compartment models the brain, skull, and scalp) is described using closed triangular meshes (see e.g. Barnard et al., 1967; Brebbia et al., 1984; Hämäläinen and Sarvas, 1989).

If the interfaces between compartments are formed of triangles, and the potential is constant within each triangle, then Eq. 2.12, with some manipulation, leads into a linear system for the unknown potential $\boldsymbol{V}$ (Hämäläinen et al., 1993):

$$\boldsymbol{V} = \boldsymbol{H}\boldsymbol{V} + \boldsymbol{g}, \qquad (2.14)$$

where $\boldsymbol{H}$ is a matrix that depends on the conductor geometry, i.e. has to be calculated only once for each conductor geometry, and $\boldsymbol{g}$ is a source term that depends on the source configuration. Instead of the constant potential approximation, the potential on

each triangle may be allowed to vary linearly or quadratically (Munck, 1992; Schlitt et al., 1995).

The electric potential is defined up to an additive constant, so Eq. 2.14 does not have a unique solution. This situation can be circumvented by deflation (Barnard et al., 1967) and the resulting equations can be solved by iterative methods such as the Gauss-Seidel algorithm. The numerical computation of $\boldsymbol{V}$ (Eq. 2.14) is quite straightforward for a one-compartment model but models that have several layers may result in large numerical errors if the situation is not handled properly. Hämäläinen and Sarvas (1989) have suggested a so-called isolated-problem approach that improves the accuracy. When the potential $\boldsymbol{V}$ has been solved, the magnetic field can be calculated using Eq. 2.11.

In addition to BEM models described here, the head can be modelled using the finite element method (FEM; Johnson, 1997; Buchner et al., 1997) where the head is divided into volume elements that can have different conductivities. With FEM models it is possible to take into account local conductivity changes, which may affect significantly the estimation of the strength of the cortical currents but not necessarily the localisation of the active area (Haueisen et al., 1997).

In the publication P1 we investigated the impact that different head conductor models (sphere models and realistically shaped BEM models) have on the accuracy of MEG source estimation.

2.4 MEG as a brain research tool

Presently, several tools for functional brain imaging are available. Because these different methods give at least partly complementary information they do not directly compete with each other but open different windows to human brain function.

MEG detects neural current flow, the very basis of information processing in the brain. With MEG it is possible to follow the brain activations at a millisecond time-scale. The most problematic feature of MEG is the source localisation that, by definition, has no unique solution. Still, as real experiments have shown, the source locations can often be found both reliably and accurately (Rose et al., 1991, Godey et al., 2001, Mäkelä et al., 2001). This aspect of MEG was also studied in this thesis (P1) with computer simulations but utilising realistic noise and source localisation procedures.

Positron emission tomography (PET) and functional MRI (fMRI) provide accurate spatial information, as they do not suffer from the non-uniqueness of the inverse problem. However, the signals they measure are based on the cell metabolism and blood flow changes, which limits the temporal resolution they can achieve considerably. Also, their spatial accuracy often has to be traded off against noise reduction.

Electroencephalography (EEG) is a technique very close to MEG. The neural origin of EEG signals is the same as for MEG. Therefore, it shares also the time resolution of MEG. However, the accurate modelling of EEG data is more demanding than with MEG as the poorly conducting skull smears the electric potentials (Nunez, 1981). EEG detects activity from currents in any orientation whereas MEG is most sensitive to the tangential components of the neural currents, i.e. MEG signals are mainly generated by neuronal activation within the fissural cortex.

MEG has mostly been used as a research tool to investigate the basic sensory functions such as vision (Brenner et al., 1975), somatosensation (Brenner et al., 1978),

and audition (Hari et al., 1980; Hari, 1990) as well as specific cognitive tasks like picture naming (Salmelin et al., 1994), sentence comprehension (Helenius et al., 1998), reading sign language (Levänen et al., 2001), and speech production (Salmelin et al., 2000b). The research is continuously spreading into new areas and the questions addressed currently in the Low Temperature Laboratory include also topics such as cortex-muscle coherence (Salenius et al., 1997; Gross et al., 2000), human mirror-neuron system (Järveläinen et al., 2001; Avikainen et al., 2002), pain (Hari et al., 1997; Juottonen et al., 2002), and attention (Vanni and Uutela, 2000).

The first clinical applications of MEG concentrated mainly on epilepsy (Barth et al., 1982; Paetau et al., 1990). However, MEG is likely to take a more prominent role also in clinical institutions with emerging applications like the presurgical mapping of cortical areas (Gallen et al., 1993; Mäkelä et al., 2001) and investigation of specific disorders such as Parkinson's disease (see e.g. Mäkelä et al., 1993; Volkmann et al., 1996; Salenius et al., 2002). With new data analysis methods such as the dynamic imaging of coherent sources (Gross et al., 2001) it is also probable that MEG can better utilise its unique combination of good spatial and excellent temporal resolution to study the cooperation of separate brain areas. In the future, MEG is also likely to be used more often together with other imaging techniques such as the fMRI and EEG in order to combine the strong points of each method and to achieve a more complete view of brain functions.

Chapter 3

The 3D topography of MEG source localisation accuracy: simulations (P1)

In study P1 we characterised the source estimation accuracy of MEG throughout the brain volume with different head conductor models. The study was done with computer simulations but, unlike most other simulation studies, it included realistic noise taken from a real MEG recording. The studied head conductor models included both spherically symmetric and realistically shaped BEM models. In addition to errors in source location, we calculated the errors in source strength and orientation. The study included also a comparison of sensor types as the errors were calculated using data measured by first-order planar gradiometers only, by magnetometers only, and by both sensor types together. The main goals of the study were to find out (i) the typical magnitude and distribution of source estimation errors encountered when analysing MEG data and (ii) the situations, where it is adequate to use a simple spherically symmetric conductor model and where a more refined realistically shaped conductor model might be needed in order to achieve a reasonable source estimation accuracy. To our knowledge, this is the first simulation study done with MEG where all these aspects, and especially the effect of realistic noise, are considered to this extent.

3.1 Introduction

The conductor model used to describe the conductivity geometry of the head affects the MEG source localisation accuracy. The spherically symmetric model is easy to create and computationally fast, which makes it an attractive alternative. Realistically shaped models offer a more accurate description of the geometry of the head than the spherically symmetric models but they are computationally slower and more difficult to create. In particular, the construction of a 3-layer realistically shaped model may require a lot of effort as bone is not clearly visible in typical MR images (Husberg, 2001). The intrinsic bias induced by the use of different conductor models can be studied with computer simulations where the effect of noise can be excluded (Fuchs et al., 1998; Crouzeix et al., 1999; Husberg, 2001). From a practical point of view, however, the effect of noise is very important, as all real measurement signals are noisy. Furthermore, realistic noise may affect the relative performance of different conductor models.

The examination of the localisation accuracy of MEG under realistic conditions is not straightforward, as one has to know the true locations of the activated brain areas. This problem has typically been addressed in three ways. The most realistic measurement situation can be achieved by utilising implanted brain electrodes as current sources (see e.g. Balish et al., 1991; Cuffin, 1996; Rose et al., 1991). Understandably this method is limited as the number and configuration of the electrodes is very restricted. Electrode distribution is more unconstrained in a phantom that is built to mimic the structure of a real head (see e.g. Leahy et al., 1998; Menninghaus et al., 1994) but even with head phantoms the number of electrodes must be relatively small and one cannot vary the source orientations freely. In

addition, the measurement situation is not as realistic as with a real subject, because only background magnetic noise from the environment and measurement hardware is present. The most versatile situation can be achieved with computer simulations where the current sources can be configured freely and a large number of possible conditions can be studied. The most problematic feature with simulations is the selection of the reference model because the results will describe the differences between the reference model and the models used in the source localisation. To get information about how conductor models will work with real MEG data, one has to use a reference model that mimics the real situation, i.e. the human head, as closely as possible. Unfortunately, this is often restricted by computational power. Also, the effect of noise has to be taken into account as realistically as possible. In study P1 this was done by adding noise that was averaged from a real MEG data file to the simulated magnetic fields.

3.2 Methods

The simulated magnetic fields were calculated for the sensor configuration of the Vectorview™ neuromagnetometer using a 3-layer realistically shaped reference conductor model that was as refined as practically possible (Husberg, 2001). In the reference model, each compartment with different conductivity, i.e. brain, skull, and scalp, was modelled with triangles having approximately 8 mm side length (Fig. 3.1).

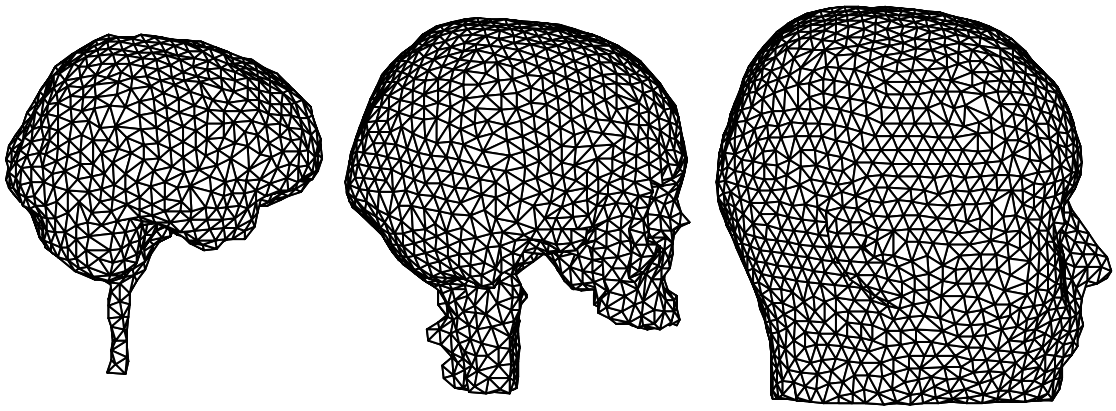

Fig. 3.1 The breakdown of the reference conductor model. From left to right, the triangle meshes describing the outer shape of brain, skull, and scalp compartments, viewed from the right (P1).

The studied brain areas, i.e. locations where the current dipoles were simulated, formed a 3-dimensional grid with a 5-mm spacing between neighbouring points, occupying the whole brain. The magnetic fields were calculated so that only one source was active at a time. To make the simulated data more realistic, noise was added to the originally noiseless magnetic fields. The noise was taken from a real MEG data file that was re-averaged (number of averages was 100) so that the new averaging times were not synchronised with the auditory stimulus presentation. The data file was recorded from a real human subject so it contained noise from the environment, the measurement hardware, and the subject. To yield different noise levels, the noise was low-pass filtered at 40 Hz or at 100 Hz. In addition, the signal-

to-noise ratio was varied using current dipoles of 15 nAm, 30 nAm, and 60 nAm as the generators of the magnetic fields. The effect of SSP noise reduction was also tested in some conditions.

From the simulated magnetic fields, the parameters of the underlying current dipoles (location, amplitude, and orientation) were estimated using the same software and techniques typically used in real data analysis. Because only one current dipole was active at a time, all the MEG sensors (typically only the gradiometers, but in some cases only magnetometers, or both gradiometers and magnetometers) were included in the source localisation. The conductor models employed in the source estimation included spherically symmetric (three models) and realistically shaped (three 1-layer models and seven 3-layer models) models that were coarser than the reference model. In spherical models the sphere origin was varied so that the BRAINSPH model matched best the overall shape of the brain compartment, FRONTSPH was fitted to the frontal brain regions and OCCISPH described best the shape of the occipital regions. In realistically shaped conductor models, the triangle sizes were varied to change the accuracy of the model. In 3-layer models this was done separately for each model compartment to test the effect that different compartments have on the functioning of the whole model. The realistically shaped models were named according to the size of the triangles used in the triangle mesh, e.g. model 1L10 was 1-layer model made of triangles with 10 mm side length whereas 3L101818 was a 3-layer model made of triangles with 10 mm side length in the brain compartment and triangles with 18 mm side length in the skull and scalp compartments.

Because Vectorview™ neuromagnetometer incorporates magnetometers and first order planar gradiometers in the same sensor locations, we were also able to compare the functioning of different sensor types by performing the source estimation using signals measured by gradiometers only, by magnetometers only, or by both sensor types together.

3.3 Results

When no noise was present, it was clear that the 3-layer realistically shaped models that resembled the reference model worked best (left column in Fig. 3.2, see also Husberg, 2001). However, the addition of even moderate levels of noise (low-pass filtered at 40 Hz) increased the source estimation errors, effectively masking the differences between different conductor models. Although realistically shaped models, especially 3-layer models, often gave the best results, the differences between conductor models were in most cases negligible (Fig. 3.2). The performance of both spherically symmetric and realistically shaped models was reasonably stable as the number of totally meaningless localisation results was small (< 2%) even with low signal-to-noise ratio (15 nAm sources).

The magnitude of source estimation errors depended heavily on the location of the activated area, which is understandable as the signal-to-noise ratio decreases when the distance to the sensors increases (Fig. 3.3). In cortical areas typically studied with MEG, i.e. in the occipital, temporal, and frontoparietal regions and in areas close to vertex, the source estimation was accurate and reliable both for spherical and realistically shaped conductor models. Here the typical location errors were within 2 – 4 mm. However, in the anterior frontal lobe and in deep structures the errors were

considerably larger, often exceeding 10 mm. The 3D topography of source amplitude and orientation errors followed closely that of location errors (Fig. 3.3).

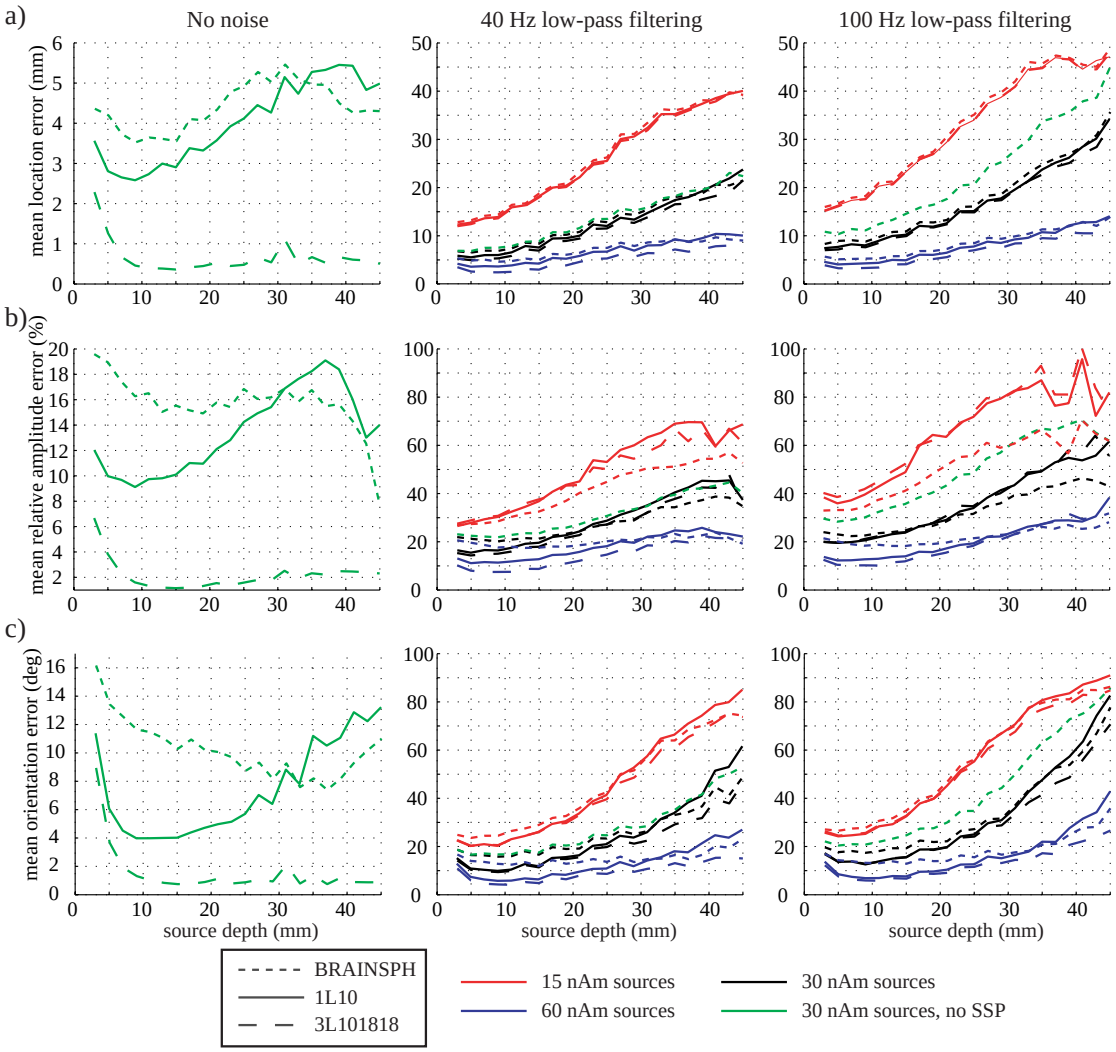

Fig. 3.2 The mean source estimation errors in a) source location, b) amplitude, and c) orientation for no noise, noise low-pass filtered at 40 Hz, and noise low-pass filtered at 100 Hz conditions (left to right) for BRAINSPH (dotted line), 1L10 (solid line), and 3L101818 (dashed line) models. The source depth is measured as the distance from the surface of the brain triangle mesh of the reference model. The line color defines the original source strength (red = 15 nAm, black = 30 nAm, and blue 60 = nAm). Green color stands for the original source strength of 30 nAm and no SSP noise reduction in the source estimation (all head models in the noiseless condition and only the BRAINSPH model in the noisy conditions). The amplitude errors are given relative to the original amplitude. Only gradiometers were used in the source estimation (P1).

The functioning of the spherical model could be slightly improved by using a sphere that was fitted to the shape of the brain area of interest. This, however, increased errors in areas far away from the primary area of interest. In 3-layer models, the size of triangles in the skull and scalp compartments did not affect the functioning

of the model as much as the size of the triangles in the brain compartment (for more details, see P1 and also Husberg, 2001).

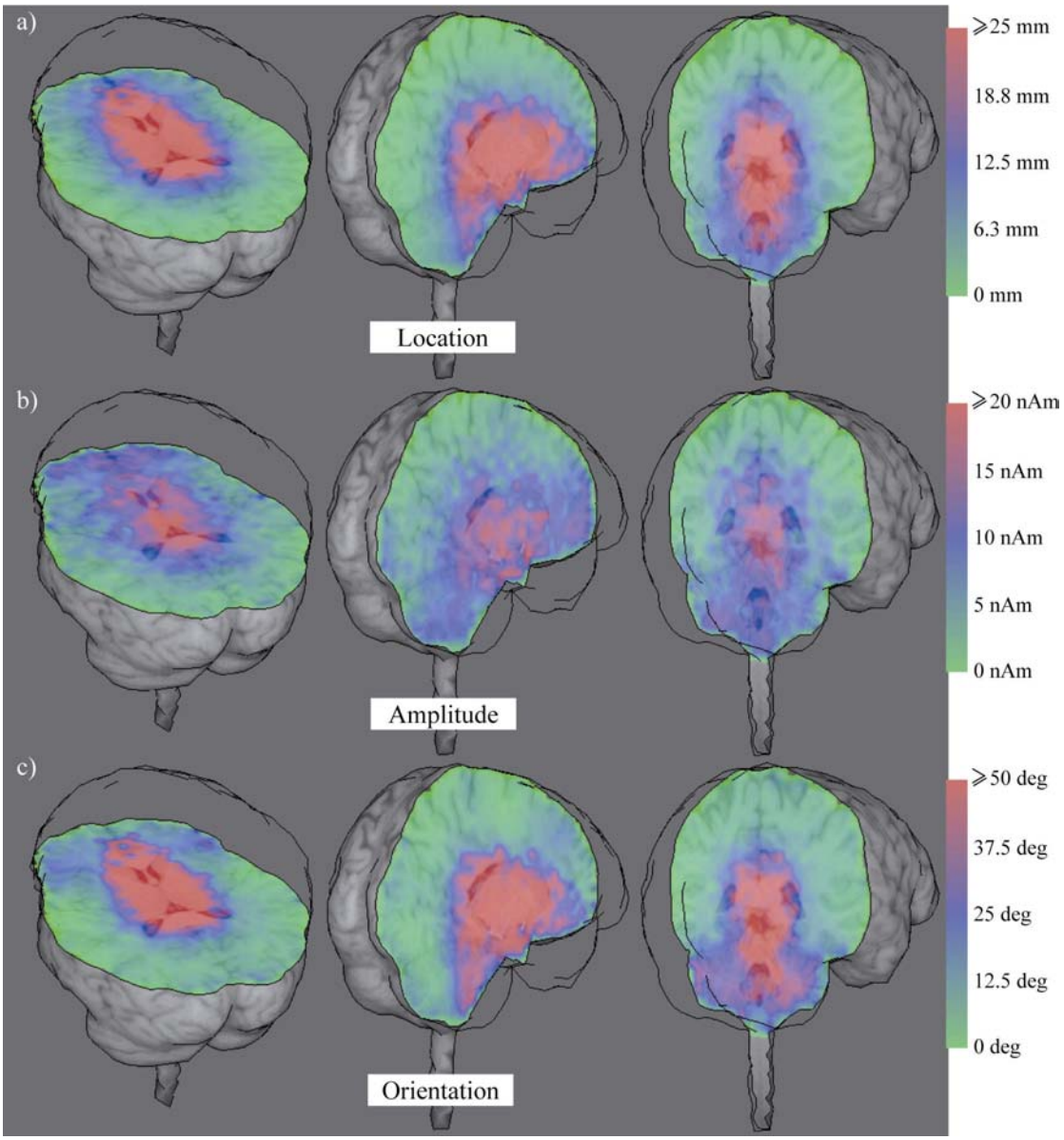

Fig. 3.3 Distribution of source estimation errors in a) source location, b) amplitude, and c) orientation using the BRAINSPH model. The original source amplitude was 30 nAm and the noise added to the simulated fields was low-pass filtered at 40 Hz (P1).

The effect of sensor type on the source estimation was considerable as gradiometers outperformed magnetometers clearly, especially in superficial source areas but also in deeper brain structures. The combined use of magnetometers and gradiometers gave results very close to the results obtained with gradiometers alone (Fig. 3.4).

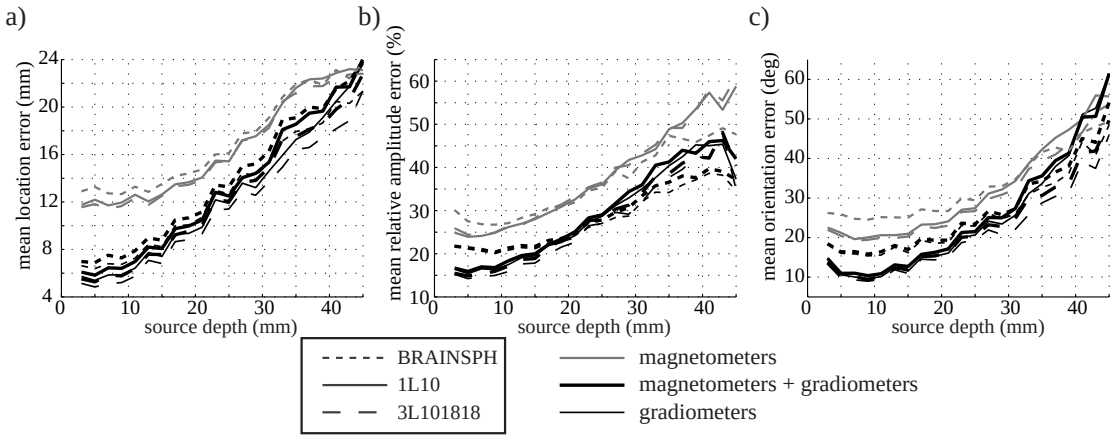

Fig. 3.4 The source estimation errors as a function of source depth in a) source location, b) amplitude, and c) orientation for MEG signals measured by magnetometers only (gray curves), by gradiometers only (thin black curves), and by the combination of magnetometers and gradiometers (thick black curves) for models BRAINSPH, 1L10, and 3L101818. The noise was low-pass filtered at 40 Hz (P1).

3.4 Conclusions

The computer simulations showed that the selection of a conductor model may not be crucial for the success of the source estimation procedure as the errors induced by the noise mask effectively the differences between different conductor models. This result is in good agreement with a recent EEG-simulation study of Vanrumste et al. (2002). With realistic signal-to-noise ratios a spherically symmetric model that is fitted to the overall shape of the brain volume appears to be adequate for most everyday source analysis requirements. If one wishes to use a model as accurate as possible, a good candidate is a highly refined 1-layer realistically shaped conductor model or a 3-layer realistically shaped model where most emphasis is placed on the accuracy of the innermost, i.e. brain, compartment.

The size of estimation errors depended heavily on the overall signal-to-noise ratio but also on the brain area. The areas traditionally studied with MEG, i.e. auditory, somatosensory, motor, and visual cortices, performed well, with location errors typically in the order of 2 – 4 mm, in accordance with previous findings (Menninghaus et al., 1994; Tomita et al., 1996; Leahy et al., 1998; Crouzeix et al., 1999), whereas the anterior frontal lobe and deeper brain structures were more problematic. When analysing the frontal brain regions, one may benefit from the use of a BEM model or a locally fitted sphere model instead of a sphere model describing the entire cranial volume. At least in study P1, the use of magnetometers did not improve the source estimation accuracy, not even with deep brain structures. This is probably due to the higher noise sensitivity of magnetometers as compared with gradiometers.

Based on the results of the study P1, any means of improving the signal-to-noise ratio, such as better shielding of external noise signals, averaging, filtering, selection of proper experimental paradigm, and SSP noise reduction, are likely to be of the highest importance when one wishes to improve the source estimation accuracy of MEG.

Chapter 4

Brain activations related to visually presented letters and faces (P2 – P6)

The processing of visual information is known to involve a multitude of cortical brain areas with different functions. However, the exact roles of these areas are still at least partly unknown. Our knowledge concerning the development of these areas as well as the reasons why they may function differently in different people is also very limited, and, as the amount of information increases, even more new and important questions are and will be asked. The purpose of the studies presented here was to add to our knowledge concerning the cortical processing of two behaviourally highly significant, but also very different types of visual stimuli, namely letters and faces.

Studies P2 and P3 investigated the brain responses related to reading in non-reading-impaired (P2) and dyslexic (P3) adult subjects. Studies P4 and P5 applied similar methods to study face processing in the same subject groups, respectively. In study P6 we analysed further the properties of early reading-related brain activations in non-reading-impaired subjects.

In these studies the main emphasis was placed on identifying and characterising the earliest stimulus-specific response patterns and on the comparison of these patterns across subject groups and face and letter-string processing. The main goals of our studies were (i) to obtain an accurate description of when and where the processing of letter-string and face information segregates into specified routes, (ii) to determine when and where the cortical processing of letter-strings starts to differ between non-reading-impaired and dyslexic subjects, (iii) to study whether the dysfunction of occipitotemporal cortex observed in dyslexic readers is limited to reading or whether it affects also other spatially and temporally highly similar cortical processes (e.g. processing of faces), and (iv) to characterise in more detail the behaviour and reactivity of the first letter-string-specific processing stage in response to letter stimuli of different types.

4.1 Introduction

4.1.1 Vision

Vision is one of the most carefully studied brain functions. Even though major advances have been made, it is still safe to say that our current knowledge is very limited.

The primary cortical areas participating in the processing of visual information are mainly located in the occipital cortex. The signals originating from the eyes are processed serially and parallelly in a multitude of areas; in macaque monkeys more than 30 heavily interconnected visual and visual-association areas have been identified (Felleman and Van Essen, 1991).

Most of the visual information originating from the retina proceeds through the lateral geniculate nuclei (LGN) of thalamus and enters the cortex at the area V1 (Brodmann area 17, also known as the striate cortex). The neurons located in V1

typically react to only very simple visual features, such as a line with a certain orientation, occurring in the very small receptive field of the neuron. In V1 the visual field is represented in a retinotopical manner, i.e. adjacent cortical points have receptive fields corresponding to adjacent parts of the visual field.

Area V1 sends signals to surrounding extrastriate areas such as V2, V3, V4, and V5, each carrying out different tasks. These hierarchically higher visual areas have typically larger receptive fields and they respond to visually more complex features than neurons in V1. They are also good examples of the functional specialisation encountered in the cortical processing of visual information – and of other modalities as well. For example, the area V4 is known to play an important role in the processing of colour information (Zeki, 1973; Zeki, 1977; Lueck et al., 1989; Bartels and Zeki, 2000) whereas V5 takes part in the processing of visual motion (Dubner and Zeki, 1971; Zeki, 1974; Zeki et al., 1991; Watson et al., 1993). With the existence of such areas it is easy to understand how only some attributes of vision may be damaged while others are still working at least relatively normally (see e.g. Damasio et al., 1980; Zihl et al., 1983; Zeki, 1990; Beckers and Zeki, 1995).

Specialisation is not limited to different attributes of visual information as areas responding specifically to certain types of visual shapes or objects have also been reported. Object groups that are shown to activate specialised cortical areas include faces (Sergent et al., 1992; Haxby et al., 1994; Bentin et al., 1996; Puce et al., 1996; Kanwisher et al., 1997; Sams et al., 1997; Gorno-Tempini et al., 1998; Swithenby et al., 1998; Allison et al., 1999; Halgren et al., 2000), letter-strings (Allison et al., 1994; Nobre et al., 1994; Puce et al., 1996; Salmelin et al., 1996; Kuriki et al., 1998), buildings (Aguirre et al., 1998; Epstein and Kanwisher, 1998; Ishai et al., 1999), and numbers (Allison et al., 1994).

Even though the visual cortical areas are heavily interconnected they can be grouped into two main processing streams. The ventral visual stream extends to occipitotemporal areas and it is considered to be important for object and form vision whereas spatial vision and motion are processed in the dorsal stream extending to parietal areas (Ungerleider and Mishkin, 1982; Mishkin et al., 1983). This division of labour has led to the names ‘what’ and ‘where’ pathways for the ventral and dorsal streams, respectively. Somewhat different roles for these two visual streams have been suggested by Goodale and Milner (1992, 1995) who proposed that the ventral stream is responsible for conscious visual perception whereas the dorsal stream is important for guiding motor actions based on visual information. Parietal brain areas are also shown to be important for the allocation of visual attention (Corbetta, 1998; Vanni and Uutela, 2000).

In the studies presented here we first identified and then investigated the behaviour of occipitotemporal cortical areas responding specifically to letters and faces.

4.1.2 Reading

Even though reading, when working properly, may seem as a simple task, it is actually a complex skill that requires smooth co-operation of several other skills including visual processing, memory, phonological processing, and attention. A dysfunction in any of these subskills or in the information transfer between them can result in a reading impairment.

Visual word recognition is considered to proceed through feature, letter, and word level subprocesses. The precise nature and cortical organization of these subprocesses

is not known (for a review of different models, see e.g. Helenius, 1999; Price, 2000). In popular dual-route models (see e.g. Coltheart, 1978; Coltheart et al., 1993) the reading is considered to proceed from visual feature analysis to the understanding of the meaning of the word (semantic activation) through two different routes depending on the type of the word being read. Familiar words are recognised directly based on their visual word form whereas unfamiliar words and non-words undergo grapheme-to-phoneme conversion where individual letters or letter-clusters are transformed into the corresponding speech sounds. The existence of two different routes for visual word recognition is supported by acquired brain disorders where reading of real words or pseudowords is selectively impaired (for reviews of acquired dyslexias, see Ellis and Young, 1988; Ellis, 1993).

The cortical locations of the different subprocesses of reading have been investigated in a multitude of functional imaging studies (reviewed e.g. in Helenius, 1999; Price, 2000). While these results differ in some aspects, it is usually considered that language processing concentrates mainly to the left hemisphere and involves a network of cortical regions. Initial feature analysis of visual stimuli takes place in the primary visual areas and letter-strings are no exception (Puce et al., 1996). Prelexical orthographic processing of letters is probably carried out in the left occipitotemporal cortex (Nobre et al., 1994; Pugh et al., 1996; Puce et al., 1996). The reports on the cortical locations of the hierarchically higher processing stages are more variable. Tasks requiring phonological processing (including grapheme-to-phoneme conversion) are shown to activate e.g. left inferior frontal cortex and left superior temporal gyrus (Pugh et al., 1996; Rumsey et al., 1997) whereas semantic processing is associated with activations of e.g. left inferior prefrontal cortex (Demb et al., 1995), left anterior temporal pole (Vandenberghe et al., 2002), and left middle and superior temporal cortices (Pugh et al., 1996; Helenius et al., 1998).

4.1.3 Developmental dyslexia

Developmental dyslexia was first reported in children in 1896 (Morgan, 1896). This language disorder is characterised by difficulties in learning to read and write in the absence of gross neurological pathology. It is typically diagnosed as a disagreement between the true reading skills and the skills that would be expected based on the individual's age, intelligence, and the reading education s/he has received.

Behavioural studies have shown that reading problems are causally related to impaired phonological skills (Bradley and Bryant, 1983; Lundberg, 1998), i.e., the ability to perceive and manipulate speech sounds, phonemes, of the spoken language and the speed of accessing phonological information from memory (Wagner and Torgesen, 1987). In addition to phonological problems dyslexic individuals are known to have difficulties in processing rapidly changing visual and auditory information (see e.g. Stein and Walsh, 1997; Tallal et al., 1998; Hari and Renvall, 2001) and they may also suffer from a number of other deficits including motor clumsiness and attention deficit disorder (reviewed in Laasonen, 2002).

For a theory of dyslexia to be ideal, it would have to be able to pinpoint a core deficit capable of explaining the different symptoms associated with dyslexia. Based on the variety of symptoms and the many different ways in which fluent reading can be impaired, it is very possible that no single cause can ever account for all the different manifestations of dyslexia. The current theories of dyslexia can be divided into three groups (reviewed in Laasonen, 2002): (i) Problems in phonological and language processing are the direct cause of developmental dyslexia and the non-

linguistic symptoms are independent of dyslexia. (ii) A more fundamental deficit, such as impaired perceptual processing, is responsible for the problems in reading acquisition. (iii) The linguistic problems and other, possibly co-existing perceptual difficulties are manifestations of a common, more profound problem. The purpose of the studies on dyslexia included in this thesis was not to decide between such theoretical accounts but to focus on the cortical correlates of impaired reading in dyslexia and, above all, to identify the earliest differences in cortical processing of letter-strings between dyslexic and non-reading-impaired subjects.

Previous functional imaging studies (reviewed in Pugh et al., 2000; Salmelin et al., 2000a) have indicated that, in particular, the posterior parts of the left hemisphere are underactivated during reading in dyslexic individuals (Salmelin et al., 1996; Shaywitz et al., 1998; Brunswick et al., 1999; Paulesu et al., 2001). MEG recordings showed that this difference between non-reading-impaired and dyslexic subjects emerges within the first 200 ms after word onset (Salmelin et al., 1996). However, the functional role of this abnormality remained uncertain. In addition, the subsequent left superior temporal activation at around 400 ms after word onset, reflecting semantic processing, was found to be delayed in dyslexic individuals (Helenius et al., 1999, 2002).

4.2 Subjects

4.2.1 Non-reading-impaired subjects

The studies P2, P4, and P6 were performed on healthy, non-reading-impaired adult readers. Studies P2 and P6 concentrated on letter-string reading and study P4 on face processing. All the subjects in these studies were right-handed Finnish-speaking university students or graduates. In the publication P2 we had 12 subjects with ages ranging from 21 to 42 years (mean age 29 years; 4 females, 8 males). In the study P4 we had 10 subjects (ages 23 – 44 years, mean age 31 years; 4 females, 6 males) who had all participated also in the study P2. The same set of subjects were studied in order to enable direct comparison of measured brain activation patterns between letter-string and face processing. The study P6 was performed on 10 subjects, of whom 6 had also participated in the earlier study P2 (ages 24 – 38 years, mean age 28 years; 4 females, 6 males).

4.2.2 Dyslexic subjects

Similarly to non-reading-impaired subjects, many of the dyslexic individuals participated both in the letter-string reading (P3) and in the face processing (P5) studies. The study P3 was performed on 10 dyslexic, Finnish speaking adults (ages 22 – 36 years, mean age 30 years; 4 females, 6 males). Six of them were able to participate also in the study P5. In addition, we recruited two new subjects to the study P5 giving a total of eight subjects (ages 25 – 35 years; mean age 31 years; 3 females, 5 males).

All these subjects had a history of developmental dyslexia diagnosed during school years. They had finished at least 2 years of formal education following the comprehensive school (9 years in Finland) indicating that their reading problems were not due to inferior intellectual capacity. With the exception of one dyslexic subject

(participating in both studies), all our subjects were right-handed. For eight subjects, there was a family history of reading problems.

We conducted a number of behavioural tests to gain better understanding of the cognitive profile of our dyslexic participants. Specifically, all dyslexic subjects were tested for oral reading speed and most of them also for word recognition speed. Reduced reading speed has been found to be a highly reliable marker for dyslexia among readers of both Finnish and German languages, which both have at least relatively regular orthography (Wimmer, 1993; Leinonen et al., 2001). Compared with the control group of non-reading-impaired individuals all our dyslexic subjects were at least 2 standard deviations (SDs) slower in oral reading or word recognition. Further details about the tests carried out on the dyslexic readers can be found in the publications P3 and P5.

4.3 Stimuli

All the stimuli were presented visually. In the studies P2 and P3 we used letter-strings and strings of geometrical symbols that were manipulated in two ways (Fig. 4.1). In the study P2 the length of a string was one, two, or four items. In the case of letter-strings, the two-letter strings were Finnish syllables and the four-letter strings legitimate Finnish nouns. The visibility of the letter-strings was varied using noise masking. Noise was added to the originally noiseless images by changing the grey level of each pixel randomly. The amount of change was picked from a Gaussian distribution with zero mean and a standard deviation corresponding to the level of noise. The level 8 affected the identification of the string only slightly, whereas level 16 made it quite difficult and level 24 almost impossible. Symbol-strings were always presented without noise. In addition to letter- and symbol-strings, the different noise levels were presented as such (pure noise in Fig. 4.1). Study P3 on dyslexic individuals utilised a smaller subset of the same stimuli as only pure noise patches and four-item symbol- and letter-strings were presented.

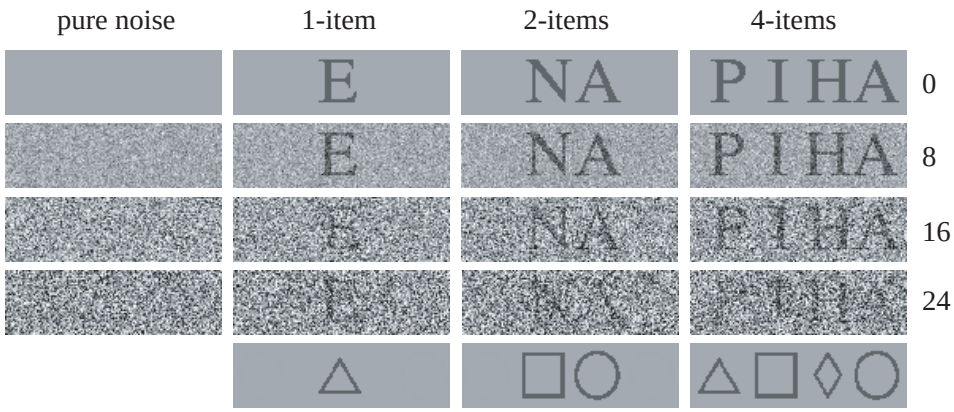

Fig. 4.1 The stimuli of study P2 consisted of 1-item, 2-item, and 4-item strings of letters or geometrical symbols. The 2-letter strings were Finnish syllables and 4-letter strings Finnish nouns. The letter-strings were masked with 4 levels of noise (0, 8, 16, 24) affecting the visibility of the string. Symbol-strings were always presented without any noise (level 0). Different noise levels were also presented as such, i.e. without the letters (pure noise).

In the study P6 the letter-string stimuli were manipulated in three ways. The length of the string was 4, 6, or 8 letters. The strings were either common Finnish nouns or meaningless consonant strings (all consonant strings were 6 letters in length) affecting the lexicality of the string. In addition, we changed the spatial demands of the reading task by shifting the letters in some of the strings vertically (Fig. 4.2).

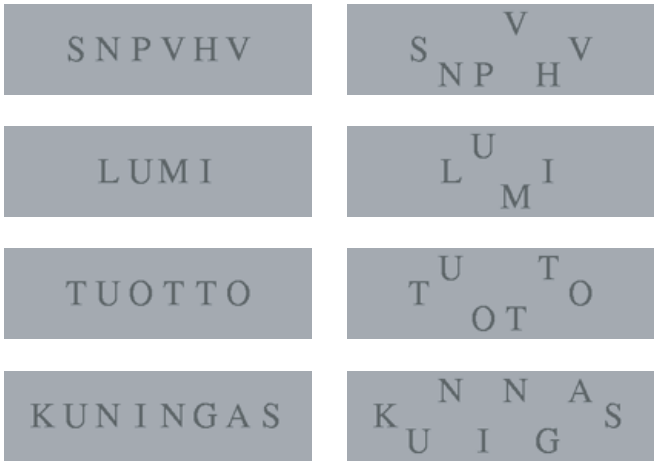

Fig. 4.2 The stimuli used in study P6 consisted of 4-, 6-, and 8-letter Finnish words and 6-letter random consonant strings written either in the normal way (left column) or by shifting the inner letters vertically by the height of a letter (right column).

Studies P4 and P5 used the same face and object stimuli (Fig. 4.3). The drawn faces were simple, cartoon-like illustrations with different expressions. Some of these images were masked with the same levels of noise as the letter-strings in studies P2 and P3. The face activations were compared to those evoked by images of common household objects and by images where the parts of the drawn faces were rotated and shifted randomly and placed inside geometrical objects to yield images that were as complex but not as easily recognized as the drawn faces. An additional comparison was based on the use of photographs depicting similar facial expressions and household objects as those seen in the drawn images.

All these stimulus sets were constructed with the following key ideas in mind. Within each experiment the stimulus set was changed along one or two variables (string length and/or string/face visibility) in a systematic way, which should make it possible to recognise brain correlates changing in a similar fashion. The sets also included stimulus contrasts that should make it possible to identify brain areas reacting to specific types of stimuli, i.e. faces vs. objects and letter-strings vs. symbol-strings. The studies comparing non-reading-impaired and dyslexic subjects (P2 vs. P3 and P4 vs. P5) used the same stimuli for both subject groups. In addition, the face and object stimuli were constructed in a way that was as similar to the letter-string and symbol-string stimuli as possible, including the use of the same grey levels in the images as well as the use of same levels of masking noise.

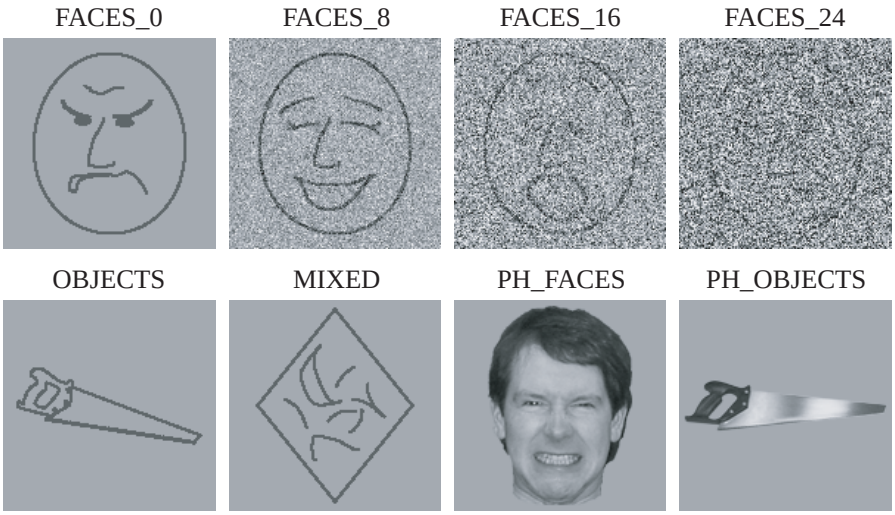

Fig. 4.3 The stimuli used in the studies P4 and P5 consisted of drawn faces with different expressions, masked with the same levels of noise as the letter-strings in the study P2 (levels 0, 8, 16, 24), of drawn images of common household objects, of mixed images where the parts of the faces (eyebrows, eyes, mouth, and nose) were rotated and shifted and placed inside geometrical objects, of black-and-white photographs of faces with expressions similar to those in the drawn images, and of black-and-white photographs of objects similar to those in the drawn images.

4.4 Recordings and data analysis

4.4.1 MEG recordings

The recordings in P2 and P3 were done with the Neuromag-122™ whole-head neuromagnetometer. Studies P4, P5, and P6 were performed with the newer 306-channel Vectorview™ system. In all our recordings the basic idea was the same. Different stimulus types were presented in a pseudo-randomised sequence on a screen in front of the subject. The images occupied a visual angle of about 2*5 degrees (letter- and symbol-strings) or of about 5*5 degrees (faces and objects) and they were presented on a grey background. The stimulus presentation was as brief as possible. The letter- and symbol-strings were displayed for 60 ms in the studies P2 and P3. The somewhat more taxing (slower to analyse) letter-strings of study P6 as well as the face and object images of studies P4 and P5 were shown for 100 ms. The consecutive images were separated by a 2-s blank interval.

The task of the subject was to pay attention to the stimuli and, when prompted by appearance of a question mark (1.5% probability), to name the letter-string or to name the expression on the face image shown just prior to the appearance of the question mark. The purpose of this task was to make sure that subjects stayed alert during the recording.

The MEG signals were band-pass filtered at 0.03 – 120 Hz and sampled at 397 Hz (P2, P3) or at 0.1 – 200 Hz and sampled at 600 Hz (P4, P5, P6). The responses evoked by each stimulus category were averaged together either online or offline. Epochs contaminated by eye movements or blinks were excluded from the averages.

Typically, the amount of averages in one category was 80 – 110. In most cases, the averaging time window, with respect to stimulus onset, was from –200 ms to 800 ms.

4.4.2 Data analysis

The averaged signals were low-pass filtered digitally at 40 Hz and analysed individually using the equivalent current dipole (ECD) approach. Each ECD representing the centre of an active cortical area was determined using the data from sensor pairs surrounding the local magnetic field maximum at the time point when visual inspection revealed a dipolar field pattern with minimum interference from other active brain areas. The ECDs were identified one at a time. Only dipoles showing a good match with the measured field pattern and a reasonable location were accepted for further analysis. The base level for the signal value was calculated from the 200-ms period preceding stimulus onset. All the data analyses were performed on signals measured by the gradiometers only. The head was approximated using a spherically symmetric conductor model.

In each study and for each subject, we were able to select a single set of dipoles capable of explaining most of the recorded brain activations in all different stimulus conditions. Thus, it was possible to directly compare the behaviour of different brain areas in response to different types of stimuli.

The averaged MEG responses (see example in Fig. 4.4) already gave a good idea of the interesting differences in the brain activation patterns. This information was utilised in defining the criteria for the detection of source areas, which react to specific aspects of the stimuli. For example, in finding areas reacting specifically to faces, we compared the face and object conditions and demanded that a source had to show significantly stronger activation for images of faces than for images of objects, or, in search for sources associated with the basic visual feature analysis, we demanded that activity had to increase with the level of noise. This classification procedure was carried out with the help of a specifically written (in Matlab; MathWorks Inc., Natick, MA, USA) visualisation algorithm that colour-coded the differences between ECD amplitude curves, with level of significance estimated from the standard deviations of the amplitude curves within the prestimulus base level interval. After identification of specific response types in each subject, these sources were grouped across subjects, and the mean activation strength, timing, and location were computed for each stimulus condition.

4.5 Activation patterns in non-reading-impaired subjects

4.5.1 Low-level visual feature analysis (P2, P4, P6)

The name Type I was originally (P2) given to the response pattern found at about 100 ms after stimulus onset in the midline occipital areas, bilaterally. The key feature of this activation pattern was its sensitivity to the level of noise masking the images: it increased systematically with the noise. An identical activation pattern was observed also with face and object stimuli (P4). The probable role of this activation is low-level visual feature analysis (VFA).

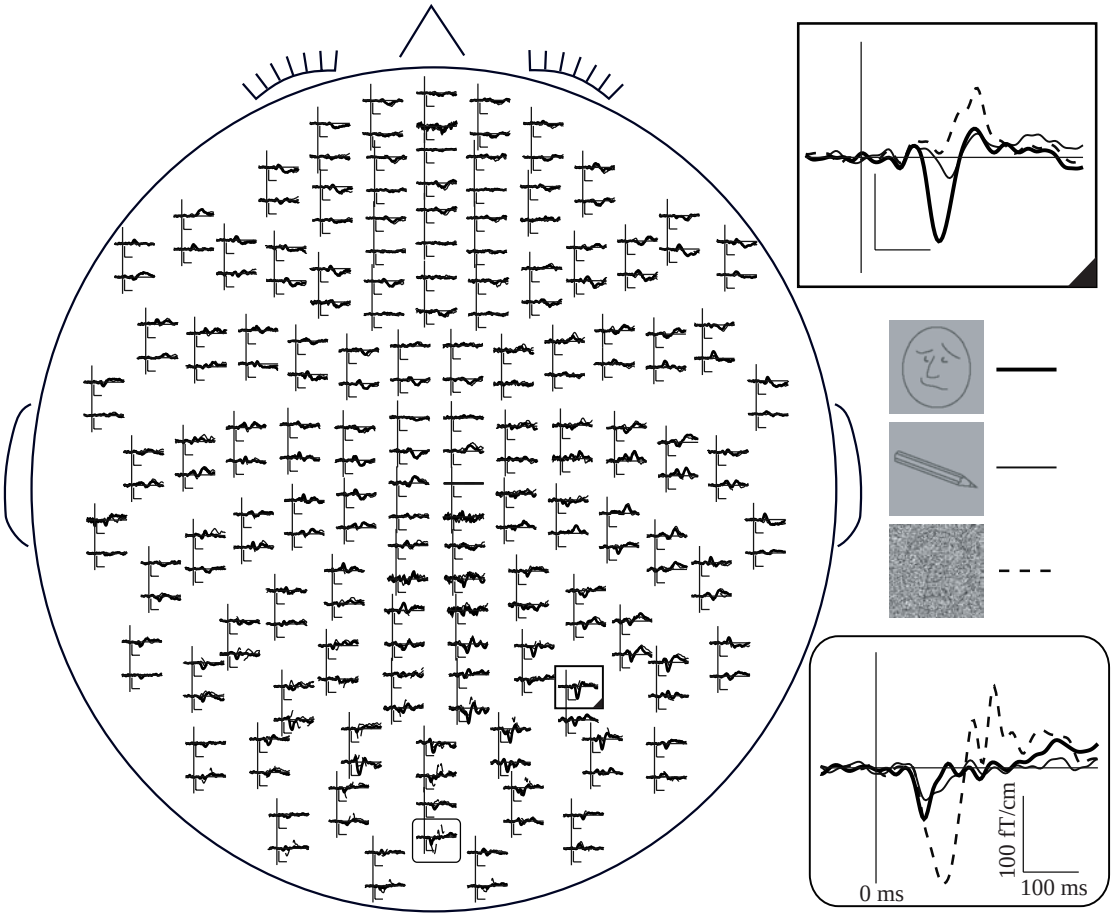

Fig. 4.4 An example of averaged brain responses from one subject in the study P4. The helmet-shaped sensor array of Vectorview™ neuromagnetometer is flattened to a plane and viewed from above with the nose pointing upwards. Only signals measured by the gradiometers are shown. These sensors measure the strongest signal just above the activated area. The enlarged sensor signals on the right illustrate two response types: the occipital midline region shows strongest activation to the heavily noise-masked images (dashed line) around 120 ms (with respect to the stimulus onset marked with the vertical line) whereas the right occipitotemporal region shows preference for images of faces (thick solid line) around 140 ms.

Cortical origin

The VFA sources were concentrated to areas bordering V1 and extended ventrally, probably as far as V4v (Fig. 4.5). The mean onset latency of VFA was about 65 ms and it peaked at about 100 ms after stimulus onset with no differences between the face (P4) and letter-string (P2) stimuli.

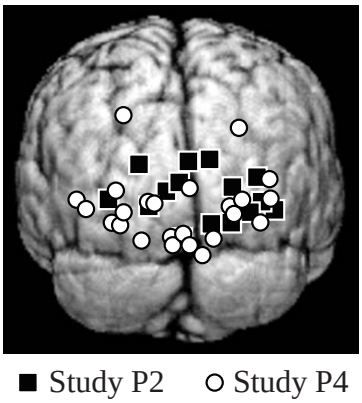

Fig. 4.5 The locations of VFA sources for letter-string (P2) and face stimuli (P4), collected from all subjects. The sources were mainly located in the occipital cortex around midline with no significant differences between the two studies.

Behaviour of VFA activation

The VFA activation increased with the amount of masking noise and the number of items (letters/symbols) in the image (Fig. 4.6) similarly for letter-string (P2) and face stimuli (P4). Accordingly, this response pattern was not sensitive to the type of stimuli but it reacted only to the visual complexity of the images, which we defined as the mean SD of the grey scale values of the stimulus images (Fig. 4.7; P4). This novel interpretation is also supported by the observation that the vertical shifts of letter position (P6) did not affect the early occipital activity.

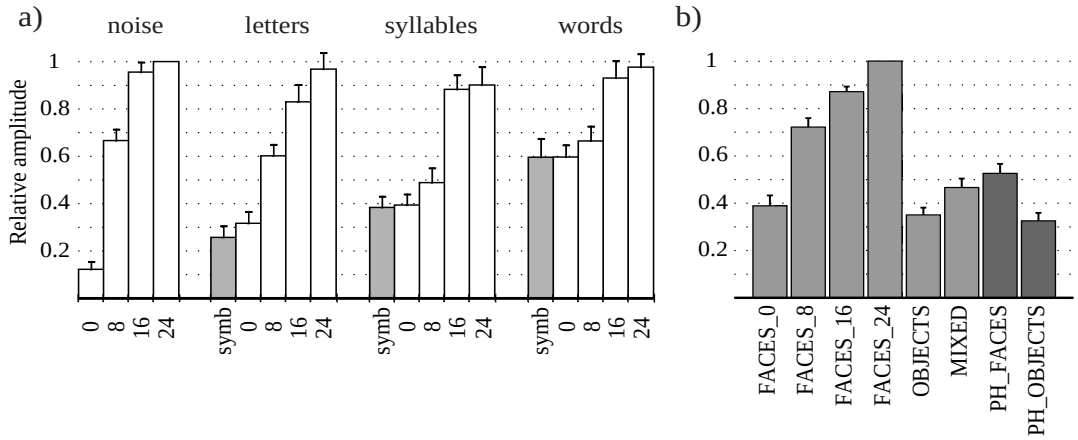

Fig. 4.6 a) The mean (+ SEM, standard error of mean) amplitudes of VFA sources reported in the study P2 were calculated relative to the noise patches with the highest level of noise (pure noise 24 -condition) and averaged across all subjects. b) The mean (+ SEM) amplitudes of VFA sources found in the study P4 are calculated relative to the faces masked with the highest level of noise (FACES_24 -condition) and averaged across all subjects. The amplitudes increased for visually more complex images (more noise or more items).

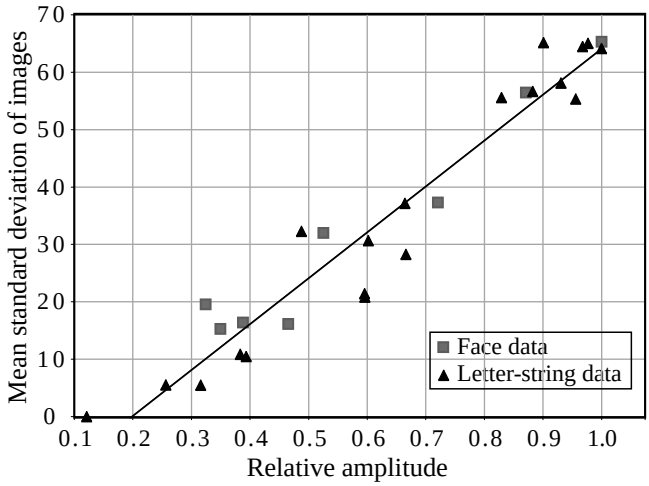

Fig. 4.7 The mean relative VFA source amplitudes correlated highly significantly ($r = 0.97$, $P < 0.00001$) with the mean visual complexity of the stimulus images (P4).

In the study P2 the VFA was shown to increase with the length of the string. However, in the study P6 the string length had no significant effect on the strength of the VFA (cType I) sources. This may seem contradictory, but is probably not. When we applied the definition of the image complexity (mean SD of grey scale values) introduced in the study P4 to the letter-string stimuli of study P6, we found that the strings of different length were actually not that far from each other (range 5 – 10). Such small differences do not predict a clear modulation of VFA (cf. Fig. 4.7). Yet, in the study P6 there was a minuscule (non-significant) increase in the VFA strength with the string length. This observation was further supported by a criterion search where a cluster of midline occipital sources showed a significantly stronger response to 8-letter than 4-letter words. For a better understanding of the VFA, it might be important to test the contributions of foveal and peripheral stimulation.

Conclusions

The probable functional role of the early occipital activation is low-level visual feature analysis, such as the extraction of oriented contrast borders, which is common to processing of both faces and letter-strings – and to other types of images as well. This interpretation is in agreement with studies reporting increased occipital activation for scrambled images (see e.g. Allison et al., 1994, 1999; Bentin et al., 1996; Halgren et al., 2000).

4.5.2 Object-level processing (P2, P4, P6)

About 30 – 50 ms after the VFA and at about 140 – 150 ms after stimulus onset, we observed responses that were specific to the type of stimulus (originally denoted as Type II activity). These responses differentiated between letter- and symbol-strings (P2) and between face and object images (P4). The activation was significantly stronger for behaviourally highly important and frequently encountered stimuli (letters, faces) than for perfectly meaningful but less important visual images (symbols, household objects).

Cortical origin

The early object-specific activation originated in the inferior occipitotemporal cortices bilaterally but with different hemispheric balance: letter-string processing showed left-hemisphere dominance whereas face processing was more bilateral with slight right-hemisphere preponderance (Fig. 4.8). Within the same hemisphere the face- (FSA) and letter-string-specific (LSA) activity was localised to immediately adjacent or overlapping occipitotemporal areas. A small but significant difference in the anterior-posterior direction suggested that the centres of face-specific source areas were on average 6 mm more anterior than the centres of letter-string-specific source areas (P4). The timing of FSA and LSA were practically identical with onset and peak latencies at about 105 ms and 140 ms, respectively.

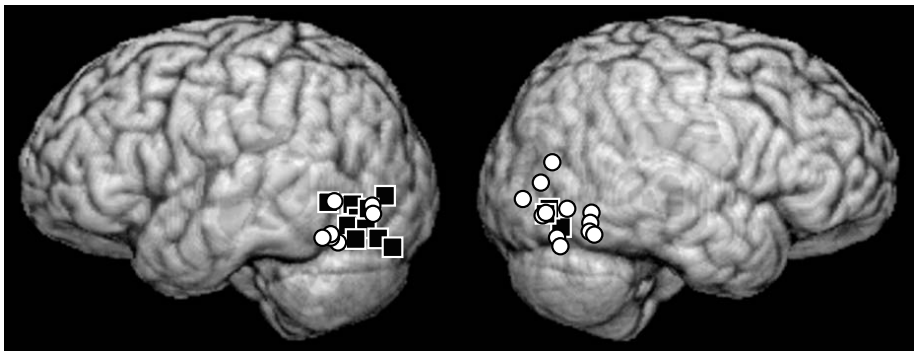

Fig. 4.8 The LSA sources were located mainly in the left inferior occipitotemporal region (P2) whereas FSA sources were distributed bilaterally with slightly more sources in the right hemisphere (P4).

Behaviour of object-specific activation

Unlike VFA activation, both LSA (P2) and FSA (P4) were severely attenuated by high levels of visual noise that made the recognition of the underlying image practically impossible (Fig. 4.9). The small increase in the strength of LSA and FSA for small levels of masking noise (Fig. 4.9) may be due to increased attention or task demand in the analysis of visually more taxing (noisy) images. However, it is noteworthy that noise in images may not always render the recognition process more difficult. In fact, the performance of a non-linear system can actually be enhanced by adding an appropriate level of noise to the input. This phenomenon is known as stochastic resonance (see e.g. Wiesenfeld and Moss, 1995; Moss and Wiesenfeld, 1995). Interestingly, visual noise has been shown to improve the recognition of low contrast images of letters (Piana et al., 2000).

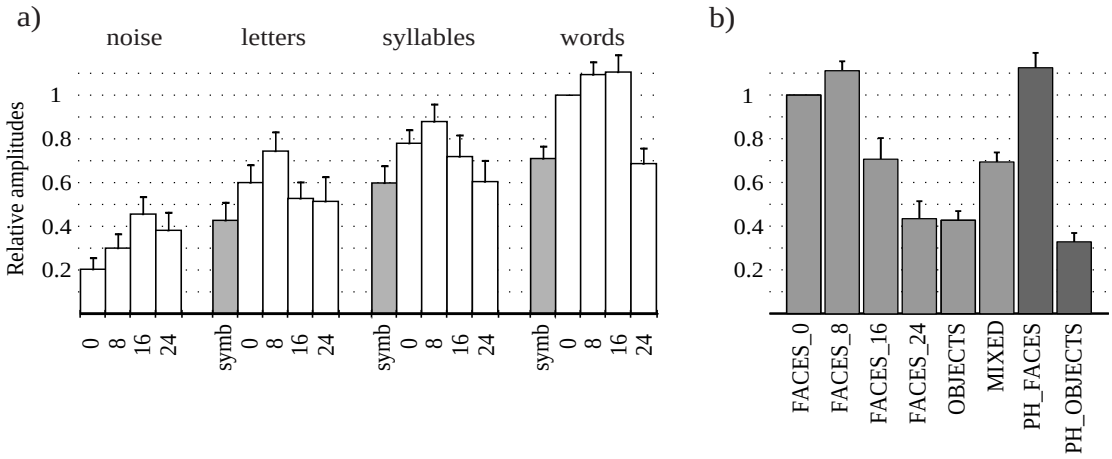

Fig. 4.9 a) The mean (+ SEM) amplitudes of LSA sources reported in the study P2 are calculated relative to the activation by 4-letter words without noise (words_0). b) The mean (+ SEM) amplitudes of FSA sources found in the study P4 are calculated relative to the activation by drawn faces without noise (FACES_0).

The FSA was stronger for images that contained parts of faces in abnormal orientations and locations (MIXED) than for fully familiar objects (Fig. 4.9b). Apparently, even a few lines that resemble parts of faces are enough to activate the early occipitotemporal face-specific neuronal populations. This supports the suggested role of these areas in the structural encoding of different face components (Eimer, 1998).

The inferior occipitotemporal LSA is prelexical as both legitimate words and readable pseudowords are known to evoke equal amounts of activity (Salmelin et al., 1996; Dehaene et al., 2002). The study P6 showed that even word-likeness is not required in the sense that random consonant strings evoked activity similar to nouns. Disturbing the normal appearance of the strings by shifting the letter positions vertically decreased the activation strength in the left occipitotemporal region slightly whereas an inverse reaction was observed in the right occipitotemporal region (P6). This evidence suggests that the early, mainly left-hemispheric LSA is tuned to seeing letters arranged in strings (as in normal print) and may be involved in computing letter-shape or letter-identity. It is thus plausible that strings of typical word length, i.e. 4 letters or more, suffice to activate this area to almost the full extent and, therefore, the increase in activity for 4 letters vs. 1 letter (P2) does not continue for longer strings (P6). The results also suggest that the right inferior occipitotemporal cortex is involved in the processing of letter- and symbol-strings but with a somewhat different role than the corresponding area in the left hemisphere. One possibility is that the left occipitotemporal cortex processes the strings at a more local level whereas the right occipitotemporal cortex concentrates on more global processing (P6).

Comparison with published literature

Our results are in good agreement with a multitude of reports showing that areas participating in the face (e.g. Sergent et al., 1992; Haxby et al., 1994; Bentin et al., 1996; Puce et al., 1996; Kanwisher et al., 1997; Sams et al., 1997; Gorno-Tempini et

al., 1998; Swithenby et al., 1998; Allison et al., 1999; Cohen et al., 2000; Halgren et al., 2000) and letter-string (e.g. Petersen et al., 1988, 1989, 1990; Price et al., 1994, 1996; Puce et al., 1996; Pugh et al., 1996; Salmelin et al., 1996; Rumsey et al., 1997; Kuriki et al., 1998) processing exist in the occipitotemporal cortices. The exact timing of this activation is, however, somewhat unsettled as some electromagnetic studies report LSA (Nobre et al., 1994; Allison et al., 1994; Salmelin et al., 1996; Cohen et al., 2000) and FSA (Allison et al., 1994; Bentin et al., 1996; Sams et al., 1997; Eimer, 1998; Halgren et al., 2000) peaking within 160 – 200 ms, i.e. somewhat later than the activity reported here. The reason for these differences may be found in the measurement conditions. Probable candidates would be the image parameters (size and luminance), presentation parameters (stimulus duration and inter-stimulus interval), and the subject's task. The most obvious candidate is stimulus duration. Our results are in agreement with Swithenby et al. (1998) who, similar to us, used a stimulus duration of 100 ms and showed face-specific MEG activation already at 140 ms after stimulus onset. MEG studies reporting face activation peaking at about 160 ms used rather long stimulus durations, 240 ms (Halgren et al., 2000) or 500 ms (Sams et al., 1997). On the other hand, the explanation may be more complex as the event-related potential studies of Schendan et al. (1998) show face activation peaking at 150 ms with a 700-ms stimulus presentation time.

Cohen et al. (2002), using fMRI, have recently suggested a rather different role for the occipitotemporal LSA. These authors reported that legitimate words activate the occipitotemporal cortex more than random consonant-strings. They suggested that this activity represents a visual word form area that is tuned to the orthographic regularities and therefore disfavours consonant-strings that violate the normal letter combination rules. The apparent discrepancy between our data (P6) and those of Cohen et al. (2002) may derive from different task parameters but also from methodological differences. First, the activity detected with MEG and fMRI may originate in different, although probably nearby, neural populations. Secondly, and probably more importantly, the variance may be accounted for by temporal differences. The activity reported in P6 took place in a short time-window around 150 ms after stimulus onset whereas the metabolic activity seen in fMRI is a summation over a longer time-window and, perhaps, over different cognitive processes. This interpretation is also supported by the earlier EEG observations of Cohen et al. (2000) where the activation difference between words and consonant-strings started to emerge only around 200 ms and continued well beyond 300 ms.

Role of attention

One specious explanation for the face and letter-string-specificity of the early occipitotemporal responses might be our task that directed the subject to pay more attention to the letter-strings (P2) or faces (P4) than to the other image categories. Wojciulik et al. (1998), using fMRI, showed that the fusiform face activation can be modulated by voluntary attention. However, attention is not likely to have a strong effect on the LSA/FSA at about 150 ms after stimulus onset as Puce et al. (1999) demonstrated that top-down influences (semantic priming and face-name learning and identification) did not affect the ventral face-specificity within 200 ms of image onset but only later in time, which supports the automatic nature of the early occipitotemporal responses. The situation is, however, far from settled as recent EEG results of Bentin et al. (2002) suggest that priming can affect the face-specific processing already at 170 ms after stimulus onset. Even if attention plays a major role in early object-specific responses, dissociation of the processing pathways obviously

occurred at about 150 ms after stimulus onset, with lateralisation to left inferior occipitotemporal cortex for attended letter-strings and more bilateral response pattern for attended faces.

Conclusions

Both the FSA and LSA are likely to represent a more general object-level processing stage that takes place after the common low-level VFA and acts as a gateway to higher processing areas. In the studies presented here, this activation was seen for faces and letter-strings, i.e. for two different classes of visual stimuli united by their importance to modern day human. The ability to recognise letter-strings and faces quickly and accurately develops through massive amounts of practice. It is thus plausible that, if needed, similar abilities can be developed also for other classes of objects. This effect was demonstrated e.g. by Allison et al. (1994), who have identified responses specific to Arabic numbers in areas close to those responding specifically to faces and letter-strings, and by Gauthier et al. (1999, 2000), who showed that the face-specific fusiform area can be activated similar to faces also by other classes of objects (a novel group called 'greebles', birds, and cars) in individuals who have had a lot of practice in recognising the objects in their field of expertise.

The remarkable spatial and temporal similarity of LSA and FSA is noteworthy as visually faces and letters are clearly distinct and, probably even more importantly, they also differ on an evolutionary scale. As reading is a relatively new skill, it is difficult to believe that it could be expressed on a genetic level. Instead, it has to be developed through extensive exposure to printed text. Face processing, on the other hand, is an evolutionary old and important skill so it is likely to have a considerable innate component, even though also face processing develops through practice (Carey, 1992; Ellis, 1992). Still, it seems that both skills use highly similar cortical systems within the visual domain.

4.6 Activation patterns in dyslexic subjects and comparison to non-reading-impaired subjects

4.6.1 Low-level visual feature analysis (P3, P5)

The early occipital activity at about 100 ms after stimulus onset, associated with low-level VFA, showed no systematic differences between the non-reading-impaired and dyslexic subjects either in the letter-string reading (P3) or in the face processing (P5) tasks. The timing, strength, behaviour, and cortical locations of the VFA sources matched well between the two subject groups, implying that this processing stage was functioning normally in the dyslexic individuals.

4.6.2 Object-level processing (P3, P5)

The early LSA in dyslexic readers differed from that in non-reading-impaired subjects. In the control group, we found letter-string-specific sources in the left inferior occipitotemporal cortex in 10/12 subjects (P2). In the dyslexic subject group, we were able to find similar sources in the same cortical area only in 2/8 subjects (Fig. 4.10a; P3). This difference was statistically significant (Fisher's exact probability test, $P < 0.008$). In addition, two dyslexic subjects had LSA sources in the left hemisphere but more than 2 SDs posterior to the mean source location of the non-reading-

impaired subjects. One dyslexic subject had two LSA sources in the right occipital area. Furthermore, the mean activation strength of the LSA sources was smaller in dyslexic than non-reading-impaired subjects for readable (noise levels 0, 8, and 16) words (Fig. 4.10b). These observations demonstrate that the earliest cortical activation showing specificity for letter-strings was abnormal in dyslexic subjects. Our result is in agreement with other MEG, fMRI, and PET reports showing that the posterior parts of the left hemisphere are underactivated during reading in dyslexic individuals (Salmelin et al., 1996; Shaywitz et al., 1998; Brunswick et al., 1999; Paulesu et al., 2001).

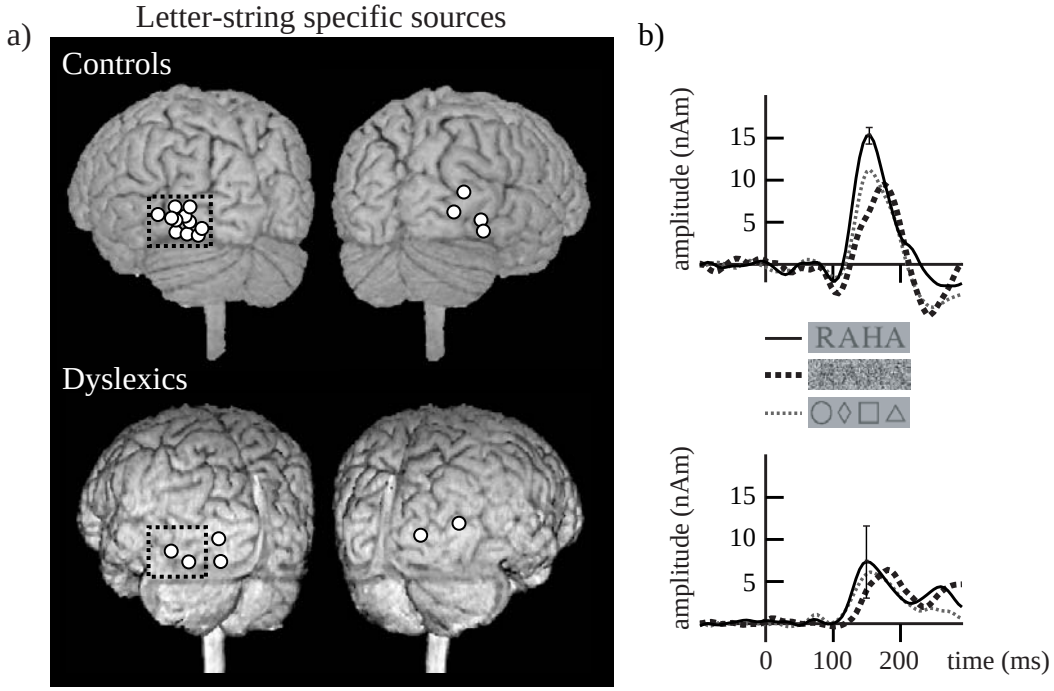

Fig. 4.10 a) The dyslexic subjects had few LSA sources and only two of them were located in the same left inferior occipitotemporal region (dashed rectangle) where non-reading-impaired subjects had all their left-hemispheric LSA sources. b) The mean amplitude curves of LSA sources show that LSA activity, when detected at all, was weaker and less robust in the dyslexic than non-reading-impaired subjects (P3).

In contrast to the letter-string processing (P3), the early occipitotemporal processing of faces was essentially normal in the dyslexic individuals (P5). The FSA was seen bilaterally at the same occipitotemporal locations in both subject groups (Fig. 4.11). The mean peak latency of the FSA at 139 ms was practically identical to that in the control subjects (142 ms). When the hemispheres were investigated separately, the left-hemispheric FSA seemed to be slightly weaker in dyslexic than non-reading-impaired subjects, but the interpretation of this result was complicated by the observation that in the left hemisphere the FSA sources were also slightly more superficial in dyslexic than control subjects ($P < 0.03$). The estimation of the exact depth of a source is somewhat error-prone in MEG. If the estimated location of the source is superficial with respect to the actual location, the source will appear weaker than it is. In other words, it is possible that the differences in source depth and activation strength are tied together and only reflect uncertainty in source estimation.

Nevertheless, the dyslexic subjects exhibited a clear FSA also in the left inferior occipitotemporal cortex that had earlier (P3) failed to separate letter- and symbol-strings. Importantly, our present findings thus suggest that the occipitotemporal impairment in dyslexic individuals is not a general one affecting all processing taking place in the same occipitotemporal region or time-window of activation around 150 ms but is likely to be limited to processing of letters or at least letter-like objects.

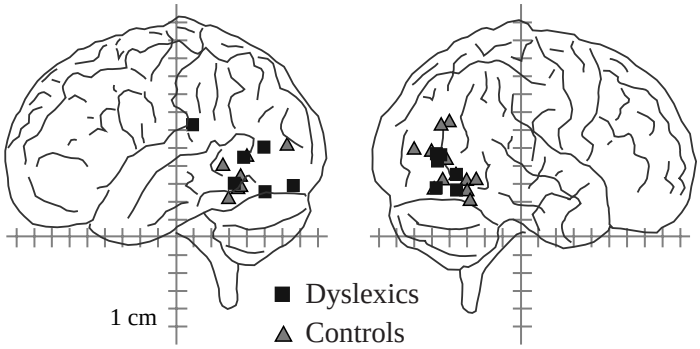

Fig. 4.11 The FSA sources were distributed in a similar way both in the dyslexic and control subjects (P5).

4.6.3 Behavioural differences

The key problem in dyslexia is slowish and error-prone reading, which was also obvious in our dyslexic subjects who were all significantly slower in oral reading and/or word recognition than age-matched controls (P3, P5). However, somewhat surprisingly we noticed clear differences also in the face and object processing abilities between the dyslexic and control groups, even though the dyslexic individuals were tested to have perfectly normal non-verbal intelligence (P5) and we observed no clear differences in the early FSA between the subject groups.

The face recognition abilities of the subjects were tested using the short version of a facial recognition test (Benton et al., 1978), and a computerized face recognition test, based on the same images, where the subject indicated by pressing a corresponding button, as quickly as possible, which of the two faces in the lower half of the computer screen represented the same individual as shown in the upper half of the screen. In addition to faces, the subjects also judged the similarity of very simple geometrical objects (e.g. triangle, circle, cross, semicircle; P5).

In the facial recognition task (Benton et al., 1978) the dyslexic subjects made more errors (mean 4.5 ± SEM 0.6) than the control group (2.3 ± 0.4; two-tailed *t*-test, $P < 0.003$). In the computerized face recognition task the dyslexic individuals (2465 ± 565 ms) were slower than control subjects (1095 ± 40 ms) in judging the similarity of faces ($P < 0.002$). The dyslexic subjects were also slower in judging the similarity of objects (430 ± 15 ms vs. 350 ± 10 ms, $P < 0.00005$). This new finding suggests that even though the early cortical processing of faces seems to be intact in dyslexic subjects, there still may be some differences between fluent and dyslexic readers in the way face and object information is being processed (see below).

4.6.4 Other activation patterns

In addition to the early visual feature analysis and the first object-level processing stage described above, we observed a number of other systematic response patterns in the face and letter-string tasks. Of these probably the most interesting was a right-hemisphere parietotemporal activation seen at 200 – 300 ms in 8/10 non-reading-impaired subjects but only in 2/8 dyslexic readers (Fig. 4.12; P5). In the control group, this response appeared with equal strength to images of both faces and household objects. The right parietotemporal activation is thus probably associated with some process that is common to both types of images. In control subjects, the timing of this activation pattern was correlated with the reaction times in the similarity-matching task (P5). Although the true nature of this parietotemporal response is not currently known, the lack of activation in dyslexic subjects and the correlation between cortical latencies and behavioural reaction times in non-reading-impaired subjects suggest that it may be related to the behavioural difference seen in face and object matching between non-reading-impaired and dyslexic subjects.

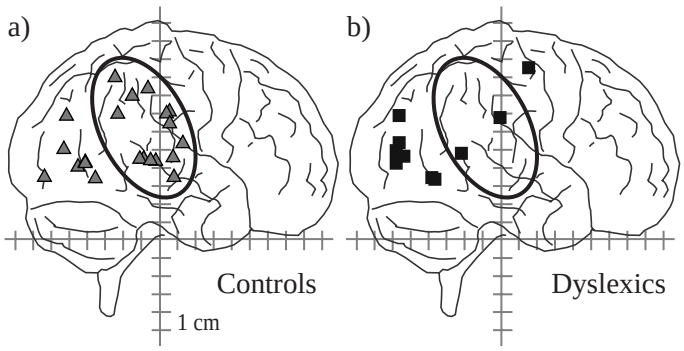

Fig. 4.12 The distribution of right-hemispheric sources that showed strongest activation 200 – 300 ms after stimulus onset differed between a) non-reading-impaired and b) dyslexic subjects in the parietotemporal region (black ellipse; $P < 0.02$) where most dyslexic readers had no sources at all (P5).

4.7 Conclusions

The early visual processing of faces and letter-strings consists of at least two distinguishable processes taking place in the occipital and occipito-temporal cortices within 200 ms after the stimulus presentation. The first process, low level visual feature analysis, took place at about 100 ms after image onset in areas surrounding the V1 cortex. This activity was not sensitive to the specific content of the stimulus, and was common to the processing of both letter-strings and faces. It showed a monotonic increase in activation strength as a function of the visual complexity of the image. Some 30 – 50 ms later and about 150 ms after stimulus onset, stimulus-specific activation emerged in the inferior occipitotemporal cortices. Although both letter-strings and faces activated largely overlapping areas in the inferior occipitotemporal cortex, the hemispheric distribution of these areas was different. Letter-string processing concentrated to the left hemisphere, whereas face processing occurred more bilaterally, with slight right-hemisphere dominance. Taking into account the visual and evolutionary differences in letter-string and face processing, it is

noteworthy that both skills utilise such similar cortical systems within the visual domain.

The letter-string-specific processing stage was not lexically sensitive. It was seen both for legitimate words and for consonant strings that violated normal rules on letter combination and relative location of letters. A plausible explanation for the observed behaviour is its participation in the coding of letter- but not word-identities. The face-specific activation did not differ significantly between processing of realistic photographs and simplified drawn images of faces. Also, drawn images where parts of faces were shifted and rotated randomly evoked stronger activity than perfectly meaningful images of objects. This supports the notion that the underlying cortical areas participate in the structural encoding of different face components (Eimer, 1998).

The problems dyslexic individuals typically report are related to fluent reading. Here, we have shown that the cortical responses between non-reading-impaired and dyslexic subjects start to differ at the level of the earliest letter-string-specific activation. The visual feature analysis as well as the early face-specific processing seem to be intact in dyslexic readers, suggesting that the abnormality is not a general one affecting all processing in the same cortical areas or in the same time-window of activation but is at least relatively specific to processing of letters or letter-like information.

The reason why occipitotemporal category-specific processing has developed at least relatively normally for faces but not for letter-strings in dyslexic individuals is not known. Because the present results do not suggest a general occipitotemporal dysfunction in dyslexic subjects, the abnormal development of letter-string-specific activation is more likely to be caused by something that separates the recognition of letter-strings from the recognition of other visual objects.

One possible explanation is a purely visual one based on the idea that letter-strings are visually unique objects that have to be dealt with in a special way. One such model was given by Farah (1990) who, based on the variety of visual disorders affecting more or less selectively the recognition of objects, suggested that object recognition may utilise mainly two different abilities. The first ability would be involved in representing multiple shapes and it would be especially important for recognition of objects that have to be decomposed into smaller parts (such as letter-strings). The second ability would deal with representing the parts themselves and it would be especially stressed during recognition of objects that are complex but are processed in a holistic manner (such as faces), i.e. without much decomposition (Farah, 1990).

It may also be that the important factor separating face and letter-string recognition is the crossmodal nature of letter-string processing. When learning to read one must not only recognize the visual form of the letter but also combine it with auditory information, i.e. with the corresponding phoneme. Due to the phonological problems apparent in poor readers (Wagner and Torgesen, 1987), letter-strings may possibly never quite establish, at least not as strongly as in fluent readers, their status as meaningful visual objects of their own kind. The importance of phonological abilities is supported by the results of Bradley and Bryant (1983) who showed that phonological training improved children's reading skills. It may also be that dyslexic individuals have a more general deficit in combining information from several modalities. This account is supported by observations showing that dyslexic children are slower than non-reading-impaired children in processing of sequential perceptual information (Laasonen et al., 2000). This difference was already visible in unimodal

tasks but it increased for multimodal tasks and was most marked in audiovisual processing (Laasonen et al., 2000).

Postword

The work presented here is a part of a long-standing project carried out in the Brain Research Unit aiming to reveal the cortical networks participating in language comprehension and production in normal function and in dysfunction. As many important questions still remain unanswered in these areas, the project is far from being finished and studies penetrating in a more detailed fashion e.g. into the response properties of the early object-level processing are likely to be rewarded. A substantial step in that direction has already been taken in the Brain Research Unit with a new study where letter-string processing is studied in young children learning to read. This study and the many studies that are likely to follow will hopefully give us a better account of the processes that make reading such an easy and effortless task for many of us and shed some light on the origin of the reading problems encountered by dyslexic individuals.

Bibliography

Aguirre GK, Zarahn E, D'Esposito M. An area within human ventral cortex sensitive to "building" stimuli: evidence and implications. Neuron 1998; 21: 373-383.

Allison T, McCarthy G, Nobre A, Puce A, Belger A. Human extrastriate visual cortex and the perception of faces, words, numbers, and colors. Cereb Cortex 1994; 4: 544-554.

Allison T, Puce A, Spencer DD, McCarthy G. Electrophysiological studies of human face perception. I: Potentials generated in occipitotemporal cortex by face and non-face stimuli. Cereb Cortex 1999; 9: 415-430.

Avikainen S, Forss N, Hari R. Modulated activation of the human SI and SII cortices during observation of hand actions. NeuroImage 2002; 15: 640-646.

Balish M, Sato S, Connaughton P, Kufta C. Localization of implanted dipoles by magnetoencephalography. Neurology 1991; 41: 1072-1076.

Barnard AC, Duck IM, Lynn MS, Timlake WP. The application of electromagnetic theory to electrocardiology. II. Numerical solution of the integral equations. Biophys J 1967; 7: 463-491.

Bartels A, Zeki S. The architecture of the colour centre in the human visual brain: new results and a review. Eur J Neurosci 2000; 12: 172-193.

Barth DS, Sutherling W, Engel J, Jr., Beatty J. Neuromagnetic localization of epileptiform spike activity in the human brain. Science 1982; 218: 891-894.

Beckers G, Zeki S. The consequences of inactivating areas V1 and V5 on visual motion perception. Brain 1995; 118: 49-60.

Bentin S, Allison T, Puce A, Perez E, McCarthy G. Electrophysiological studies of face perception in humans. J Cogn Neurosci 1996; 8: 551-565.

Bentin S, Sagiv N, Mecklinger A, Friederici A, von Cramon YD. Priming visual face-processing mechanisms: electrophysiological evidence. Psychol Sci 2002; 13: 190-193.

Benton AL, Sivan AB, Hamsher KdS, Varney NR, Spreen O. Facial Recognition - Stimulus and Multiple Choice Pictures. New York: Oxford University Press, Inc., 1978.

Bradley L, Bryant PE. Categorizing sounds and learning to read - a causal connection. Nature 1983; 301: 419-421.

Brebbia CA, Telles JCF, Wrobel LC. Boundary element techniques: Springer Verlag, 1984.

Brenner D, Williamson SJ, Kaufman L. Visually evoked magnetic fields of the human brain. Science 1975; 190: 480-482.

Brenner D, Lipton J, Kaufman L, Williamson SJ. Somatically evoked magnetic fields of the human brain. Science 1978; 199: 81-83.

Brunswick N, McCrory E, Price CJ, Frith CD, Frith U. Explicit and implicit processing of words and pseudowords by adult developmental dyslexics: A search for Wernicke's Wortschatz? Brain 1999; 122: 1901-1917.

Buchner H, Knoll G, Fuchs M, Rienacker A, Beckmann R, Wagner M, et al. Inverse localization of electric dipole current sources in finite element models of the human head. Electroencephalogr Clin Neurophysiol 1997; 102: 267-278.

Carey S. Becoming a face expert. Philos Trans R Soc Lond [Biol] 1992; 335: 95-103.

Chapman RM, Ilmoniemi RJ, Barbanera S, Romani GL. Selective localization of alpha brain activity with neuromagnetic measurements. Electroencephalogr Clin Neurophysiol 1984; 58: 569-572.

Cohen L, Dehaene S, Naccache L, Lehericy S, Dehaene-Lambertz G, Henaff MA, et al. The visual word form area: spatial and temporal characterization of an initial stage of reading in normal subjects and posterior split-brain patients. Brain 2000; 123: 291-307.

Cohen L, Lehericy S, Chochon F, Lemer C, Rivaud S, Dehaene S. Language-specific tuning of visual cortex? Functional properties of the Visual Word Form Area. Brain 2002; 125: 1054-1069.

Coltheart M. Lexical access in simple reading tasks. In: Underwood G, editor. Strategies of information processing. New York: Academic Press, 1978: 151-216.

Coltheart M, Curtis B, Atkins P, Haller M. Models of reading aloud: dual-route and parallel-distributed-processing approaches. Psychol Rev 1993; 100: 589-608.

Corbetta M. Frontoparietal cortical networks for directing attention and the eye to visual locations: identical, independent, or overlapping neural systems? Proc Natl Acad Sci USA 1998; 95: 831-838.

Crouzeix A, Yvert B, Bertrand O, Pernier J. An evaluation of dipole reconstruction accuracy with spherical and realistic head models in MEG. Clin Neurophysiol 1999; 110: 2176-2188.

Cuffin BN. EEG localization accuracy improvements using realistically shaped head models. IEEE Trans Biomed Eng 1996; 43: 299-303.

Dale A, Sereno M. Improved localization of cortical activity by combining EEG and MEG with MRI cortical surface reconstruction: A linear approach. J Cogn Neurosci 1993; 5: 162-176.

Damasio A, Yamada T, Damasio H, Corbett J, McKee J. Central achromatopsia: behavioral, anatomic, and physiologic aspects. Neurology 1980; 30: 1064-1071.

Dehaene S, Le Clec HG, Poline JB, Le Bihan D, Cohen L. The visual word form area: a prelexical representation of visual words in the fusiform gyrus. Neuroreport 2002; 13: 321-325.

Demb JB, Desmond JE, Wagner AD, Vaidya CJ, Glover GH, Gabrieli JD. Semantic encoding and retrieval in the left inferior prefrontal cortex: a functional MRI study of task difficulty and process specificity. J Neurosci 1995; 15: 5870-5878.

Dubner R, Zeki SM. Response properties and receptive fields of cells in an anatomically defined region of the superior temporal sulcus in the monkey. Brain Res 1971; 35: 528-532.

Eimer M. Does the face-specific N170 component reflect the activity of a specialized eye processor? Neuroreport 1998; 9: 2945-2948.

Ellis AW, Young AW. Human cognitive neuropsychology. Hillsdale, NJ: Lawrence Erlbaum Associates, 1988.

Ellis AW. Reading, writing and dyslexia: A cognitive analysis. Hove: Lawrence Erlbaum Associates, 1993.

Ellis HD. The development of face processing skills. Philos Trans R Soc Lond [Biol] 1992; 335: 105-111.

Epstein R, Kanwisher N. A cortical representation of the local visual environment. Nature 1998; 392: 598-601.

Farah MJ. Visual agnosia: Disorders of object recognition and what they tell us about normal vision. Cambridge, MA: MIT Press, 1990.

Felleman DJ, Van Essen DC. Distributed hierarchical processing in the primate cerebral cortex. Cereb Cortex 1991; 1: 1-47.

Fuchs M, Drenckhahn R, Wischmann HA, Wagner M. An improved boundary element method for realistic volume-conductor modeling. IEEE Trans Biomed Eng 1998; 45: 980-997.

Gallen CC, Sobel DF, Waltz T, Aung M, Copeland B, Schwartz BJ, et al. Noninvasive presurgical neuromagnetic mapping of somatosensory cortex. Neurosurgery 1993; 33: 260-268.

Gauthier I, Tarr MJ, Anderson AW, Skudlarski P, Gore JC. Activation of the middle fusiform 'face area' increases with expertise in recognizing novel objects. Nature Neurosci 1999; 2: 568-573.

Gauthier I, Skudlarski P, Gore JC, Anderson AW. Expertise for cars and birds recruits brain areas involved in face recognition. Nature Neurosci 2000; 3: 191-197.

Geselowitz DB. On bioelectric potentials in an inhomogeneous volume conductor. Biophys J 1967; 7: 1-11.

Geselowitz DB. On the magnetic field generated outside an inhomogeneous volume conductor by internal current sources. IEEE Trans Magn 1970; 6: 346-347.

Godey B, Schwartz D, de Graaf JB, Chauvel P, Liegeois-Chauvel C. Neuromagnetic source localization of auditory evoked fields and intracerebral evoked potentials: a comparison of data in the same patients. Clin Neurophysiol 2001; 112: 1850-1859.

Goodale MA, Milner AD. Separate visual pathways for perception and action. Trends Neurosci 1992; 15: 20-25.

Gorno-Tempini ML, Price CJ, Josephs O, Vandenberghe R, Cappa SF, Kapur N, et al. The neural systems sustaining face and proper-name processing. Brain 1998; 121: 2103-2118.

Gorodnitsky IF, George JS, Rao BD. Neuromagnetic source imaging with FOCUSS: a recursive weighted minimum norm algorithm. Electroencephalogr Clin Neurophysiol 1995; 95: 231-251.

Gross J, Ioannides AA. Linear transformations of data space in MEG. Phys Med Biol 1999; 44: 2081-2097.

Gross J, Tass PA, Salenius S, Hari R, Freund HJ, Schnitzler A. Cortico-muscular synchronization during isometric muscle contraction in humans as revealed by magnetoencephalography. J Physiol 2000; 527: 623-631.

Gross J, Kujala J, Hämäläinen M, Timmermann L, Schnitzler A, Salmelin R. Dynamic imaging of coherent sources: Studying neural interactions in the human brain. Proc Natl Acad Sci USA 2001; 98: 694-699.

Halgren E, Raij T, Marinkovic K, Jousmäki V, Hari R. Cognitive response profile of the human fusiform face area as determined by MEG. Cereb Cortex 2000; 10: 69-81.

Hämäläinen MS, Sarvas J. Realistic conductivity geometry model of the human head for interpretation of neuromagnetic data. IEEE Trans Biomed Eng 1989; 36: 165-171.

Hämäläinen M, Hari R, Ilmoniemi RJ, Knuutila J, Lounasmaa OV. Magnetoencephalography - theory, instrumentation, and applications to noninvasive studies of the working human brain. Rev Mod Phys 1993; 65: 413-497.

Hämäläinen MS, Ilmoniemi RJ. Interpreting magnetic fields of the brain: minimum norm estimates. Med Biol Eng Comput 1994; 32: 35-42.

Hari R, Aittoniemi K, Järvinen ML, Katila T, Varpula T. Auditory evoked transient and sustained magnetic fields of the human brain. Localization of neural generators. Exp Brain Res 1980; 40: 237-240.

Hari R. The neuromagnetic method in the study of the human auditory cortex. In: Grandori F, Hoke M and Romani GL, editors. Auditory Evoked Magnetic Fields and Electric Potentials. Vol 6 of Advances in Audiology. Basel: Karger, 1990: 222-282.

Hari R, Salmelin R. Human cortical oscillations: a neuromagnetic view through the skull. Trends Neurosci 1997; 20: 44-49.

Hari R, Portin K, Kettenmann B, Jousmäki V, Kobal G. Right-hemisphere preponderance of responses to painful CO2 stimulation of the human nasal mucosa. Pain 1997; 72: 145-151.

Hari R. Magnetoencephalography as a tool of clinical neurophysiology. In: Niedermeyer E and Lopes da Silva F, editors. Electroencephalography: Basic Principles, Clinical Applications, and Related Fields: Williams & Wilkins, 1999: 1107-1134.

Hari R, Renvall H. Impaired processing of rapid stimulus sequences in dyslexia. Trends Cogn Sci 2001; 5: 525-532.

Haueisen J, Ramon C, Eiselt M, Brauer H, Nowak H. Influence of tissue resistivities on neuromagnetic fields and electric potentials studied with a finite element model of the head. IEEE Trans Biomed Eng 1997; 44: 727-735.

Haxby JV, Horwitz B, Ungerleider LG, Maisog JM, Pietrini P, Grady CL. The functional organization of human extrastriate cortex: a PET-rCBF study of selective attention to faces and locations. J Neurosci 1994; 14: 6336-6353.

Helenius P, Salmelin R, Service E, Connolly JF. Distinct time courses of word and context comprehension in the left temporal cortex. Brain 1998; 121: 1133-1142.

Helenius P. Neuromagnetic and psychoacoustical correlates of impaired reading and abnormal sound sequence processing in developmental dyslexia. Department of Psychology. Helsinki: University of Helsinki (Finland), 1999.

Helenius P, Salmelin R, Service E, Connolly J. Semantic cortical activation in dyslexic readers. J Cogn Neurosci 1999; 11: 535-550.

Helenius P, Salmelin R, Service E, Connolly JF, Leinonen S, Lyytinen H. Cortical activation during spoken-word segmentation in nonreading-impaired and dyslexic adults. J Neurosci 2002; 22: 2936-2944.

Helmholtz Hv. Ueber einige Gesetze der Vertheilung elektrischer Ströme in körperlichen Leitern, mit Anwendung auf die thierisch-elektrischen Versuche. Ann Phys Chem 1853; 89: 211-233, 353-377.

Holmlund C, Keipi M, Meinander T, Penttinen A, Seppä H. Novel concepts in magnetic shielding. In: Nenonen J, Ilmoniemi RJ and Katila T, editors. Biomag2000, 12th International Conference on Biomagnetism. Helsinki University of Technology, Espoo, Finland, 2001: 968-969.

Husberg M. The use of a three-layer boundary-element model in localization of brain activity. Special assignment Tfy-99.298, Department of Engineering Physics and Mathematics. Espoo: Helsinki University of Technology (Finland), 2001.

Ioannides A, Bolton J, Clarke C. Continuous probabilistic solutions to the biomagnetic inverse problem. Inverse Problems 1990; 6: 523-542.

Ishai A, Ungerleider LG, Martin A, Schouten JL, Haxby JV. Distributed representation of objects in the human ventral visual pathway. Proc Natl Acad Sci USA 1999; 96: 9379-9384.

Iversen LL. The chemistry of the brain. Sci Am 1979; 241: 134-149.

Järveläinen J, Schürmann M, Avikainen S, Hari R. Stronger reactivity of the human primary motor cortex during observation of live rather than video motor acts. Neuroreport 2001; 12: 3493-3495.

Johnson CR. Computational and numerical methods for bioelectric field problems. Crit Rev Biomed Eng 1997; 25: 1-81.

Josephson BD. Possible new effects in superconductive tunneling. Phys Lett 1962; 1: 251-253.

Jousmäki V. Artifacts in Neuromagnetic Data Studies of Somatosensory Signals and Multisensory Interactions. Department of Applied Physics. Kuopio: University of Kuopio (Finland), 1998.

Juottonen K, Gockel M, Silén T, Hurri H, Hari R, Forss N. Altered central sensorimotor processing in patients with complex regional pain syndrome. Pain 2002; 98: 315-323.

Kanwisher N, McDermott J, Chun MM. The fusiform face area: a module in human extrastriate cortex specialized for face perception. J Neurosci 1997; 17: 4302-4311.

Kelhä VO, Pukki JM, Peltonen RS, Penttinen AJ, Ilmoniemi RJ, Heino JJ. Design, construction, and performance of a large-volume magnetic shields. IEEE Trans Magn 1982; MAG-18: 260-270.

Knuutila JET, Ahonen AI, Hämäläinen MS, Kajola MJ, Laine PP, Lounasmaa OV, et al. A 122-channel whole-cortex SQUID system for measuring the brain's magnetic fields. IEEE Trans Magn 1993; 29: 3315-3320.

Kuriki S, Takeuchi F, Hirata Y. Neural processing of words in the human extrastriate visual cortex. Cogn Brain Res 1998; 6: 193-203.

Laasonen M, Tomma-Halme J, Lahti-Nuuttila P, Service E, Virsu V. Rate of information segregation in developmentally dyslexic children. Brain Lang 2000; 75: 66-81.

Laasonen M. Temporal acuity in developmental dyslexia across the life span: Tactile, auditory, visual, and crossmodal estimations. Department of Psychology. Helsinki: University of Helsinki (Finland), 2002.

Leahy RM, Mosher JC, Spencer ME, Huang MX, Lewine JD. A study of dipole localization accuracy for MEG and EEG using a human skull phantom. Electroencephalogr Clin Neurophysiol 1998; 107: 159-173.

Leinonen S, Müller K, Leppänen PHT, Aro M, Ahonen T, Lyytinen H. Heterogeneity in adult dyslexic readers: Relating processing skills to the speed and accuracy of oral text reading. Read Writ 2001; 14: 265-296.

Levänen S, Uutela K, Salenius S, Hari R. Cortical representation of sign language: comparison of deaf signers and hearing non-signers. Cereb Cortex 2001; 11: 506-512.

Lueck CJ, Zeki S, Friston KJ, Deiber MP, Cope P, Cunningham VJ, et al. The colour centre in the cerebral cortex of man. Nature 1989; 340: 386-389.

Lundberg I. Why is learning to read a hard task for some children. Scand J Psychol 1998; 39: 155-157.

Mäkelä JP, Hari P, Karhu J, Salmelin R, Teräväinen H. Suppression of magnetic mu rhythm during parkinsonian tremor. Brain Res 1993; 617: 189-193.

Mäkelä JP, Kirveskari E, Seppä M, Hämäläinen M, Forss N, Avikainen S, et al. Three-dimensional integration of brain anatomy and function to facilitate intraoperative navigation around the sensorimotor strip. Hum Brain Mapping 2001; 12: 180-192.

Menninghaus E, Lütkenhöner B, Gonzalez SL. Localization of a dipolar source in a skull phantom: realistic versus spherical model. IEEE Trans Biomed Eng 1994; 41: 986-989.

Milner DA, Goodale MA. The visual brain in action. Oxford: Oxford University Press, 1995.
Mishkin M, Ungerleider LG, Macko KA. Object vision and spatial vision: two cortical pathways. Trends Neurosci 1983; 6: 414-417.
Morgan WP. A case of congenital word blindness. Br Med J 1896; 2: 1378.
Mosher JC, Leahy RM. Source localization using recursively applied and projected (RAP) MUSIC. IEEE Trans Signal Processing 1999; 47: 332-340.
Moss F, Wiesenfeld K. The benefits of background noise. Sci Am 1995; 273: 66-69.
Munck JCd. A linear discretization of the volume conductor boundary integral equation using analytically integrated elements. IEEE Trans Biomed Eng 1992; 39: 986-990.
Nobre AC, Allison T, McCarthy G. Word recognition in the human inferior temporal lobe. Nature 1994; 372: 260-263.
Nunez PL. Electric Fields of the Brain. New York: Oxford University Press, 1981.
Paetau R, Kajola M, Hari R. Magnetoencephalography in the study of epilepsy. Neurophysiol Clin 1990; 20: 169-187.
Pascual-Marqui RD, Michel CM, Lehmann D. Low resolution electromagnetic tomography: a new method for localizing electrical activity in the brain. Int J Psychophysiol 1994; 18: 49-65.
Paulesu E, Démonet J-F, Fazio F, McCrory E, Chanoine V, Brunswick N, et al. Dyslexia: Cultural diversity and biological unity. Science 2001; 291: 2165-2167.
Petersen SE, Fox PT, Posner MI, Mintun M, Raichle ME. Positron emission tomographic studies of the cortical anatomy of single-word processing. Nature 1988; 331: 585-589.
Petersen SE, Fox PT, Posner MI, Mintun M, Raichle ME. Positron emission tomographic studies of the processing of single words. J Cogn Neurosci 1989; 1: 153-170.
Petersen SE, Fox PT, Snyder AZ, Raichle ME. Activation of extrastriate and frontal cortical areas by visual words and word-like stimuli. Science 1990; 249: 1041-1044.
Piana M, Canfora M, Riani M. Role of noise in image processing by the human perceptive system. Phys Rev E 2000; 62: 1104-1109.
Price CJ, Wise RJ, Watson JD, Patterson K, Howard D, Frackowiak RS. Brain activity during reading. The effects of exposure duration and task. Brain 1994; 117: 1255-1269.
Price CJ, Moore CJ, Frackowiak RS. The effect of varying stimulus rate and duration on brain activity during reading. NeuroImage 1996; 3: 40-52.
Price CJ. The anatomy of language: contributions from functional neuroimaging. J Anat 2000; 197: 335-359.
Puce A, Allison T, Asgari M, Gore JC, McCarthy G. Differential sensitivity of human visual cortex to faces, letterstrings, and textures: a functional magnetic resonance imaging study. J Neurosci 1996; 16: 5205-5215.
Puce A, Allison T, McCarthy G. Electrophysiological studies of human face perception. III: Effects of top-down processing on face-specific potentials. Cereb Cortex 1999; 9: 445-458.
Pugh KR, Shaywitz BA, Shaywitz SE, Constable RT, Skudlarski P, Fulbright RK, et al. Cerebral organization of component processes in reading. Brain 1996; 119: 1221-1238.

Pugh KR, Mencl WE, Jenner AR, Katz L, Frost SJ, Lee JR, et al. Functional neuroimaging studies of reading and reading disability (developmental dyslexia). Ment Retard Dev Disabil Res Rev 2000; 6: 207-213.

Rose DF, Sato S, Ducla-Soares E, Kufta CV. Magnetoencephalographic localization of subdural dipoles in a patient with temporal lobe epilepsy. Epilepsia 1991; 32: 635-641.

Rumsey JM, Horwitz B, Donohue BC, Nace K, Maisog JM, Andreason P. Phonological and orthographic components of word recognition. A PET-rCBF study. Brain 1997; 120: 739-759.

Ryhänen T, Seppä H, Ilmoniemi R, Knuutila J. SQUID magnetometers for low-frequency applications. J Low Temp Phys 1989; 76: 287-386.

Salenius S, Kajola M, Thompson WL, Kosslyn S, Hari R. Reactivity of magnetic parieto-occipital alpha rhythm during visual imagery. Electroencephalogr Clin Neurophysiol 1995; 95: 453-462.

Salenius S, Portin K, Kajola M, Salmelin R, Hari R. Cortical control of human motoneuron firing during isometric contraction. J Neurophysiol 1997; 77: 3401-3405.

Salenius S, Avikainen S, Kaakkola S, Hari R, Brown P. Defective cortical drive to muscle in Parkinson's disease and its improvement with levodopa. Brain 2002; 125: 491-500.

Salmelin R, Hari R. Spatiotemporal characteristics of sensorimotor neuromagnetic rhythms related to thumb movement. Neuroscience 1994; 60: 537-550.

Salmelin R, Hari R, Lounasmaa OV, Sams M. Dynamics of brain activation during picture naming. Nature 1994; 368: 463-465.

Salmelin R, Service E, Kiesilä P, Uutela K, Salonen O. Impaired visual word processing in dyslexia revealed with magnetoencephalography. Ann Neurol 1996; 40: 157-162.

Salmelin R, Helenius P, Service E. Neurophysiology of fluent and impaired reading: A magnetoencephalographic approach. J Clin Neurophysiol 2000a; 17: 163-174.

Salmelin R, Schnitzler A, Schmitz F, Freund HJ. Single word reading in developmental stutterers and fluent speakers. Brain 2000b; 123: 1184-1202.

Sams M, Hietanen JK, Hari R, Ilmoniemi RJ, Lounasmaa OV. Face-specific responses from the human inferior occipito-temporal cortex. Neuroscience 1997; 77: 49-55.

Schendan HE, Ganis G, Kutas M. Neurophysiological evidence for visual perceptual categorization of words and faces within 150 ms. Psychophysiology 1998; 35: 240-251.

Schlitt HA, Heller L, Aaron R, Best E, Ranken DM. Evaluation of boundary element methods for the EEG forward problem: effect of linear interpolation. IEEE Trans Biomed Eng 1995; 42: 52-58.

Sergent J, Ohta S, MacDonald B. Functional neuroanatomy of face and object processing. A positron emission tomography study. Brain 1992; 115: 15-36.

Shaywitz S, Shaywitz B, Pugh K, Fulbright R, Constable R, Mencl W, et al. Functional disruption in the organization of the brain for reading in dyslexia. Proc Natl Acad Sci USA 1998; 95: 2636-2641.

Stein J, Walsh V. To see but not to read; the magnocellular theory of dyslexia. Trends Neurosci 1997; 20: 147-152.

Swithenby SJ, Bailey AJ, Bräutigam S, Josephs OE, Jousmäki V, Tesche CD. Neural processing of human faces: a magnetoencephalographic study. Exp Brain Res 1998; 118: 501-510.

Tallal P, Merzenich MM, Miller S, Jenkins W. Language learning impairments: integrating basic science, technology, and remediation. Exp Brain Res 1998; 123: 210-219.
Tomita S, Kajihara S, Kondo Y, Yoshida Y, Shibata K, Kado H. Influence of head model in biomagnetic source localization. Brain Topogr 1996; 8: 337-340.
Tuomisto T, Hari R, Katila T, Poutanen T, Varpula T. Studies of auditory evoked magnetic and electric responses: Modality specificity and modelling. Nuovo Cimento D 1983; 2: 471-483.
Ungerleider LG, Mishkin M. Two cortical visual systems. In: Ingle DJ, Goodale MA and Mansfield RJW, editors. The analysis of visual behavior. Cambridge: MIT Press, 1982: 549-586.
Uusitalo MA, Ilmoniemi RJ. Signal-space projection method for separating MEG or EEG into components. Med Biol Eng Comput 1997; 35: 135-140.
Uutela K, Hämäläinen M, Somersalo E. Visualization of magnetoencephalographic data using minimum current estimates. NeuroImage 1999; 10: 173-180.
Uutela K, Taulu S, Hämäläinen M. Detecting and correcting for head movements in neuromagnetic measurements. NeuroImage 2001; 14: 1424-1431.
Vandenberghe R, Nobre AC, Price CJ. The response of left temporal cortex to sentences. J Cogn Neurosci 2002; 14: 550-560.
Vanni S, Uutela K. Foveal attention modulates responses to peripheral stimuli. J Neurophysiol 2000; 83: 2443-2452.
Vanrumste B, Van Hoey G, Van de Walle R, D'Have MR, Lemahieu IA, Boon PA. Comparison of performance of spherical and realistic head models in dipole localization from noisy EEG. Med Eng Phys 2002; 24: 403-418.
Volkmann J, Joliot M, Mogilner A, Ioannides AA, Lado F, Fazzini E, et al. Central motor loop oscillations in parkinsonian resting tremor revealed by magnetoencephalography. Neurology 1996; 46: 1359-1370.
Wagner RK, Torgesen JK. The nature of phonological processing and its causal role in the acquisition of reading skills. Psychol Bull 1987; 101: 192-212.
Watson JD, Myers R, Frackowiak RS, Hajnal JV, Woods RP, Mazziotta JC, et al. Area V5 of the human brain: evidence from a combined study using positron emission tomography and magnetic resonance imaging. Cereb Cortex 1993; 3: 79-94.
Wiesenfeld K, Moss F. Stochastic resonance and the benefits of noise: from ice ages to crayfish and SQUIDs. Nature 1995; 373: 33-36.
Williams RW, Herrup K. The control of neuron number. Annu Rev Neurosci 1988; 11: 423-453.
Williamson SJ, Kaufman L. Biomagnetism. J Magn Magn Mat 1981; 22: 129-201.
Wimmer H. Characteristics of developmental dyslexia in a regular writing system. Appl Psycholing 1993; 14: 1-33.
Wojciulik E, Kanwisher N, Driver J. Covert visual attention modulates face-specific activity in the human fusiform gyrus: fMRI study. J Neurophysiol 1998; 79: 1574-1578.
Zeki SM. Colour coding in rhesus monkey prestriate cortex. Brain Res 1973; 53: 422-427.
Zeki SM. Functional organization of a visual area in the posterior bank of the superior temporal sulcus of the rhesus monkey. J Physiol 1974; 236: 549-573.
Zeki SM. Colour coding in the superior temporal sulcus of rhesus monkey visual cortex. Proc R Soc Lond B Biol Sci 1977; 197: 195-223.
Zeki S. A century of cerebral achromatopsia. Brain 1990; 113: 1721-1777.

Zeki S, Watson JD, Lueck CJ, Friston KJ, Kennard C, Frackowiak RS. A direct demonstration of functional specialization in human visual cortex. J Neurosci 1991; 11: 641-649.

Zihl J, von Cramon D, Mai N. Selective disturbance of movement vision after bilateral brain damage. Brain 1983; 106: 313-340.

Zimmerman JE, Silver AH. Macroscopic quantum interference effects through superconducting point contacts. Phys Rev 1966; 141: 367-375.